

Corso di Laurea Magistrale in Fisica

A NEW HYBRID SCHEME FOR THE
TREATMENT OF HEAVY QUARKS
IN PERTURBATIVE QCD

Relatore Interno:

Prof. Stefano Forte

Relatore Esterno:

Prof. Stefano Pozzorini

Tesi di:

Davide Napoletano

matricola 826320

codice PACS 12.38.-t

Anno Accademico 2013-2014

Abstract

Calculations of high energy processes involving the production of bottom quarks, are typically performed in two different ways. One option, the *massive* or the 4F scheme, is an effective theory where the heavy quark are decoupled, which is a valid approximation for energy of the same order of that of the bottom mass.

Alternatively, one may face the situation where the typical scale of the process Q is way higher than the bottom mass. Then one can consider a scheme where the towers of $\log^m Q^2/m_b^2$, appearing from the collinear splittings, are explicitly re-summed via the Altarelli-Parisi equations into a b -PDF. This scheme is referred to the *massless* or 5F scheme.

At fixed order n in perturbation theory, the difference among these schemes amount to adding $O(\alpha_S^{n+1})$ higher-order term.

We, instead, propose a *hybrid* scheme, called the *doped* scheme, which accounts for the particular cases in which neither the 4F scheme or the 5F seems to be perfectly reliable. In this work we study the properties of this peculiar scheme. We state three conditions under which we say that the doped scheme provides reliable predictions, and we check this conditions against numerical simulations using Sherpa+OpenLoops.

Contents

1	Fundamentals of QCD	17
1.1	The QCD running coupling	17
1.2	The DGLAP equations	18
1.3	The NLO solution of the DGLAP equations	21
2	Comparing the 4F and the 5F scheme	23
2.1	Analytical comparison between the 4F and the 5F scheme	23
2.2	Some interesting processes	26
2.3	$Wb\bar{b}$ production at LHC	28
2.4	$Zb\bar{b}$ production at LHC	30
3	The doped scheme	33
3.1	The <i>doped</i> PDF set	34
3.2	Some analytical properties of the doped scheme	36
3.3	Consistency of the doped scheme	37
3.4	The $O(\alpha_S^{N+2})$ terms	38
4	Comparing the doped scheme with the 4F and the 5F scheme	43
4.1	$Wb\bar{b}$ production at LHC	43
4.2	$Zb\bar{b}$ production at LHC	47
5	A NNLO analysis	51
6	Conclusions	55
	Appendices	57
A	The splitting functions and the anomalous dimensions	59
B	Computation of the massless limit	61
	Bibliography	67

List of Figures

1.1	Diagrams contributing to the QCD β function	17
2.1	The different running of $\alpha_S(Q^2)$ in the 4F(blue) and in the 5F(red) scheme (the large figure) and the ratio between the two (small figure). Note that here we assume that in the schemes the value of the coupling coincides at the bottom mass.	27
2.2	Diagram contributing to $pp \rightarrow Wb\bar{b}$	28
2.3	Differential distributions for $Wb\bar{b}$ production with respect to the p_T of the W boson(bottom), of the leading p_T jet (top right) or of the invariant mass of the b -jet pair (top left), in the 4F(green) and the 5F(red) scheme. The uncertainty band is that of the Monte-Carlo integration.	29
2.4	Diagrams contributing to $pp \rightarrow Zb\bar{b}$	30
2.5	Same as fig. (2.3) but for $Zb\bar{b}$ production.	31
3.1	Ratio of the gluon density in the 5F(red) and in the doped(black) scheme at $Q^2 = 10, 10^2$ and 10^3 GeV ² with respect to the 4F scheme (green).	35
4.1	Differential distributions for $Wb\bar{b}$ production with respect to the p_T of the W boson(bottom), of the leading p_T jet (top right) or of the invariant mass of the b -jet pair (top left), in the 4F(green), in the 5F(red) and in the doped scheme(black). The uncertainty band is that of the Monte-Carlo integration. Numerical results are obtained with $p_T^{cut} > 25$ GeV.	44
4.2	Same as fig. (4.1) with $p_T^{cut} > 5$ GeV.	45

-
- 4.3 Differential distributions for $Zb\bar{b}$ production with respect to the p_T of the Z boson(bottom), of the leading p_T jet (top right) or of the invariant mass of the b -jet pair (top left), in the 4F(green), in the 5F(red)and in the doped scheme(black). The uncertainty band is that of the Monte-Carlo integration. Numerical results are obtained with $p_T^{cut} > 25$ GeV. 48
- 4.4 Same as fig. (4.3) but with $p_T^{cut} > 5$ GeV. 49

List of Tables

2.1	NLO total cross sections for $Wb\bar{b}$ at $\sqrt{s} = 7$ TeV. Each scheme is computed at $\mu_R = \mu_F = M_W + 2m_b$. The error shown is that of the Monte-Carlo integration.	30
2.2	NLO total cross sections for $Zb\bar{b}$ at $\sqrt{s} = 7$ TeV. Each scheme is computed at $\mu_R = \mu_F = M_Z + 2m_b$. The error shown is that of the Monte-Carlo integration.	31
4.1	NLO cross sections for $Wb\bar{b}$ at $\sqrt{s} = 7$ TeV. Each scheme is computed at $\mu_R = \mu_F = M_W + 2m_b$. The errors shown are the Monte-Carlo errors.	43
4.2	$h^{(0)}, g^{(0)}, \bar{h}, \bar{g}$ values for $Wb\bar{b}$ production.	46
4.3	NLO cross sections for $Zb\bar{b}$ at $\sqrt{s} = 7$ TeV. Each scheme is computed at $\mu_R = \mu_F = M_Z + 2m_b$. The errors shown are the Monte-Carlo error.	47
4.4	$h^{(0)}, g^{(0)}, \bar{h}, \bar{g}$ values for $Zb\bar{b}$ production.	50
B.1	$\Delta(i, j, Q^2, m_b^2)$ at NLO for $p_T^{cut} > 25$ GeV	63
B.2	$\Delta(i, j, Q^2, m_b^2)$ at NLO for $p_T^{cut} > 5$ GeV	64

Introduction

The accurate description of hadron-hadron collisions is of increasing importance at the LHC. Due to the recent discovery of a Higgs-like boson, it will be very important to have a better control over third generation quark initiated process, since they have the highest masses among all quark and, hence, they interact most strongly with the electroweak symmetry breaking sector in the Standard Model (SM).

Theoretical predictions in QCD have been obtained according to a variety of schemes for dealing with heavy quark masses. Two classes of schemes can be adopted for dealing with heavy quark distributions. One is called the massless scheme (5F henceforth) the other is called the massive scheme (4F). In the latter scheme, heavy quarks (*e. g.* the bottom and the top quark) appear only as final state particles and they are not associated with a PDF, while in the former scheme collinear logarithms arising from collinear splittings are re-summed to all orders into a heavy quark PDF. The advantage of a 4F scheme is that heavy quarks are treated as massive, thus calculations in the 4F scheme are meant to provide reliable results when the typical scale of the process is not much larger than the mass of the heavy quark m , whereas, at any finite order in a perturbation theory, they are expected to break down as the scale becomes large compared to the mass of the heavy quark. On the other hand, since heavy quarks are treated as massless, calculation in the 5F scheme are usually much easier and provide reliable results for scales much higher than the heavy quark mass.

Both the 4F and the 5F can be included in a Fixed Flavor Number Scheme (FFNS) or in their natural extensions called Variable Flavor Number Schemes (VFNS), which consists of a sequence of n_f -flavor FFNS, each in its region of validity, consistently matched at transition thresholds. The simplest implementation of the VFNS is the Zero-Mass (ZM) approximation, where all quarks are treated as massless. Heavy quarks are absent (or infinitively massive) at scales $\mu^2 < m^2$, and they are radiatively generated (as massless) above the transition point $\mu^2 = m^2$ by the sub-process $g \rightarrow q\bar{q}$. Since, basically, the only mass effects are due to the change the number of flavors in the β function and in the splitting functions (or theirs Mellin space transformed *Anomalous dimensions*) as one cross the heavy

quark thresholds, the ZM formalism is expected not to be a good approximation in the region near the physical threshold. However, powers of m^2/Q^2 can also be consistently included at higher orders. This schemes are called General-Mass VFNS. All partons, including the bottom and the top quark are associated with a PDF above their respective threshold. The GM-VFNS represents an improvement with respect to the ZM-VFNS. However, it also introduces new ambiguities regarding the shifting of higher-order terms into the lower-order expression. In the GM-VFNS the mass of the heavy quark is taken into account in the partonic cross sections, and the scheme is constructed to interpolate between the FFN scheme, which holds a correct description of the threshold region, and the ZM-VFNS which accounts for large energy logarithms.

The first proposed matching technique for the inclusion of mass suppressed terms was developed long ago; it is the so-called ACOT scheme [4]. It yields the complete quark mass dependence from the low to the high energy regime, providing manifest decoupling for $Q^2 \gg m^2$ whereas reducing precisely, in the limit $Q^2 \ll m^2$, to the correct $\overline{\text{MS}}$ scheme. Several variants of this method were subsequently proposed, such as S-ACOT [28] or ACOT- χ [37].

A different approach, the Thorne-Roberts [36] VFN scheme or TR' [35] in its latest version, includes higher-order terms to ensure the correct threshold behavior and in order to smooth the function at the transition point. Namely the NLO calculation, which includes $O(\alpha_S^2)$ terms, which formally belong to the NNLO and they are introduced so to cure the discontinuities of the physical observables at the heavy quark mass threshold.

Another way to solve the problem is to consider both massless and massive scheme calculations as power expansion in the strong coupling constant and to replace the coefficients of the expansion in the former with their exact massive counterpart in the latter. This is the so-called FONLL [13] scheme introduced in the context of hadro-production of heavy quarks, and recently applied to Deeply Inelastic Scattering (DIS) [23].

Most of the up-to-date PDF sets [8, 9, 32, 29, 2] adopt one of the schemes pictured above as the default scheme. On top of that they usually also provide a FFNS parton set with $n_f = 3, 4, 5$.

At fixed order n in perturbation theory, the difference among these schemes amount to adding $O(\alpha_S^{n+1})$ higher-order term. Therefore this difference is reduced increasing the perturbative order (a benchmark comparison has been made to NNLO and is available in [5]).

As stated in [30], however, there are many cases of current interest in which the effects of initial state logs are rarely very large in hadron collision at the LHC. Hence, in this cases, 4F scheme computations are perturbatively well behaved and a substantial agreement between predictions computed in the 4F and in the 5F

scheme is found. The reason for this behavior is found to be that the re-summation of the initial state logarithms into the b -PDF is relevant only at large Bjorken x and the, possibly, large ratios Q^2/m_b^2 are always accompanied by universal phase space suppression factors. The authors also suggest that one should use both schemes so to exploit their complementary advantages for different observables.

From a purely phenomenological viewpoint, though, one can ask whether using the 4F scheme is a good choice, since it underestimates the value of the coupling constant (and hence that of the various observables) especially at high energies or for processes which start with a large power of α_S , even in those cases where the contribution coming from collinear splitting logarithms can be negligible. In view of this argument we propose a *hybrid* scheme, called the *doped* scheme, which accounts for this particular cases. In order to do this, the doped scheme is defined as to be exactly equal to the 4F one except for the running of the coupling which is computed in the 5F scheme.

This thesis is organized as follows. In the first chapter we review the fundamental tools that will be use throughout the rest of this work, setting the notation. In chapter 2 we will show a comparison between the 4F and the 5F scheme, with reference to $W/Zb\bar{b}$ production. In the last part of this work we will present the *doped* scheme and discuss its analytical properties. Finally we present a numerical comparison of this scheme with the usual 4F and 5F scheme again with specific reference to $W/Zb\bar{b}$ production.

Chapter 1

Fundamentals of QCD

In this chapter we will review some fundamental aspects of QCD, setting the notation used throughout the rest of this work. We will also report some results, which will be useful in the following chapters, which are not usually shown in standard references. In this work we expect the reader to be familiar with quantum field theory in general and QCD in particular.

1.1 The QCD running coupling

We recall that the QCD *running coupling* $\alpha_S(\mu^2)$, is defined as

$$(1.1) \quad \frac{\partial \alpha_S(\mu^2)}{\partial \log \mu^2} = \beta(\alpha_S),$$

where the β function has a perturbative expansion

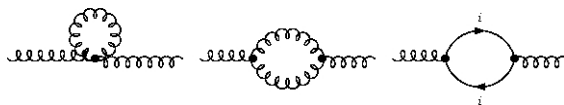


Figure 1.1: Diagrams contributing to the QCD β function

$$(1.2) \quad \beta(\alpha_S) = -b_0 \alpha_S^2 (1 + b_1 \alpha_S + O(\alpha_S^2)),$$

so that

$$(1.3) \quad \frac{\partial \alpha_S(\mu^2)}{\partial \log \mu^2} = -b_0 \alpha_S^2 (1 + b_1 \alpha_S + O(\alpha_S^2)),$$

where

$$(1.4) \quad b_0 = \frac{(33 - 2n_f)}{12\pi}, \quad b_1 = \frac{(153 - 19n_f)}{2\pi(33 - 2n_f)}.$$

We also recall that the LO, or one loop, solution of eq. (1.5) is

$$(1.5) \quad \alpha_S(\mu^2) = \frac{\alpha_S(\mu_0^2)}{1 + \alpha_S(\mu_0^2)b_0 \log \frac{\mu^2}{\mu_0^2}}.$$

Since it is going to be useful in the following let us write the $O(\alpha_S^3)$ expansion of the LO solution of the re-normalization group equation,

$$(1.6) \quad \alpha_S(\mu^2) = \alpha_S(\mu_0^2) \left(1 - \alpha_S(\mu_0^2)b_0 \log \frac{\mu^2}{\mu_0^2} + \alpha_S^2(\mu_0^2)b_0^2 \log^2 \frac{\mu^2}{\mu_0^2} + O(\alpha_S^3) \right).$$

The NLO solution of eq. (1.5), can also be found in analytical form once the LO one is known,

$$(1.7) \quad \alpha_S(\mu^2) = \frac{\alpha_S(\mu_0^2)}{1 + \alpha_S(\mu_0^2)b_0 \log \frac{\mu^2}{\mu_0^2}} \left[1 - b_1 \frac{\alpha_S(\mu_0^2)}{1 + \alpha_S(\mu_0^2)b_0 \log \frac{\mu^2}{\mu_0^2}} \log \left(1 + b_0 \alpha_S(\mu_0^2) \log \frac{\mu^2}{\mu_0^2} \right) \right],$$

this in turn can be expanded in power of α_S yielding, up to $O(\alpha_S^4)$ terms,

$$(1.8) \quad \alpha_S(\mu^2) = \alpha_S(\mu_0^2) \left[1 - \alpha_S(\mu_0^2)b_0 \log \frac{\mu^2}{\mu_0^2} + \alpha_S^2(\mu_0^2)b_0 \log \frac{\mu^2}{\mu_0^2} \left(b_0 \log \frac{\mu^2}{\mu_0^2} - b_1 \right) + O(\alpha_S^3) \right].$$

1.2 The DGLAP equations

We also recall that the DGLAP equations [6], in x space, read

$$(1.9) \quad \frac{\partial f_i^{(n_f)}(x, \mu^2)}{\partial \log \mu^2} = \frac{\alpha_S^{(n_f)}(\mu^2)}{2\pi} \sum_j \int_x^1 \frac{dy}{y} P_{ij}^{(n_f)} \left(\frac{x}{y}, \alpha_S^{(n_f)}(\mu^2) \right) f_j^{(n_f)}(y, \mu^2)$$

where i runs from zero to the number of light active flavour, n_f . The P_{ij} s are the well known Altarelli-Parisi's splitting functions. They are calculable as a power series in α_S ,

$$(1.10) \quad P_{ij}^{(n_f)}(z, \alpha_S^{(n_f)}) = P_{ij}^{(n_f),(0)}(z) + \frac{\alpha_S^{(n_f)}}{2\pi} P_{ij}^{(n_f),(1)} + \dots$$

and

$$(1.11) \quad P_{ij}^{(n_f),(0)}(z) = \begin{pmatrix} p_{qq}^{(0)}(z) & p_{qg}^{(0)}(z) \\ p_{gq}^{(0)}(z) & p_{gg}^{(n_f),(0)}(z) \end{pmatrix}$$

and we will give their full expression in the appendix. These functions provide the probability for an initial state parton i to split into a parton j , accordingly to the theory's allowed vertex.

We will now obtain the $O(\alpha_S^2)$ expression for the LO solution of the DGLAP equations. In doing so, we will follow the notation used in [24]. Let us first recall that the DGLAP equation can be written, in Mellin space as:

$$(1.12) \quad \frac{df_i^{(n_f)}(N, \tau^{(n_f)})}{d\tau^{(n_f)}} = \gamma_{ij}^{(n_f)}(N, \tau^{(n_f)}) f_j^{(n_f)}(N, \tau^{(n_f)})$$

where:

$$(1.13) \quad f_i^{(n_f)}(N, \tau^{(n_f)}) = \int_0^\infty dx x^{N-1} f_i^{(n_f)}(x, \tau^{(n_f)}), \quad \gamma_{ij}^{(n_f)}(N, \tau^{(n_f)}) = \int_0^\infty dx x^{N-1} P_{ij}^{(n_f)}(x, \tau^{(n_f)})$$

and $\tau^{(n_f)}$ is defined as:

$$(1.14) \quad \tau^{(n_f)} \equiv \frac{1}{2\pi} \int_{t_0}^t dt' \alpha_S^{(n_f)}(t').$$

Then the renormalization group equation, can be re-written in terms of τ :

$$(1.15) \quad \frac{d\alpha_S(\tau)}{d\tau} = -b_0\alpha_S(1 + b_1\alpha_S + \dots).$$

As the Altarelli-Parisi splittings, the anomalous dimensions admit an α_S expansion,

$$(1.16) \quad \gamma_{ij}^{(n_f)}(N, \tau^{(n_f)}) = \gamma_{ij}^{(n_f),(0)}(N) + \alpha_S^{(n_f)}(\tau^{(n_f)}) \gamma_{ij}^{(n_f),(1)}(N) + \dots$$

where

$$(1.17) \quad \gamma_{ij}^{(n_f),(0)}(N) = \begin{pmatrix} \gamma_{qq}^{(0)}(N) & \gamma_{qg}^{(0)}(N) \\ \gamma_{gq}^{(0)}(N) & \gamma_{gg}^{(n_f),(0)}(N) \end{pmatrix}$$

and their explicit expression is given in the appendix. We can thus, perturbatively, find the solution to eq. (1.12),

$$(1.18) \quad \frac{df_i^{(n_f)}(N, \tau^{(n_f)})}{d\tau^{(n_f)}} = \gamma_{ij}^{(n_f),(0)}(N) f_j^{(n_f)}(N, \tau^{(n_f)}) + \dots$$

To solve this system we first note that $\det \gamma_{ij}^{(0)} \neq 0$ and that $\gamma_{ij}^{(0)}$ has n_f distinct eigenvalues. This means that we can always find a matrix R such that $\det R \neq 0$ and

$$(1.19) \quad R_{im}^{(-1)} \gamma_{mn}^{(0)} R_{nj} = \lambda_i \delta_{ij},$$

where λ_m are the eigenvalues of the matrix γ_{mn} and R is the eigenvector matrix. Note that the matrix R is not uniquely defined. This is due to the fact that eigenvectors are defined up to a multiplicative factor. This means that one can find another matrix, say \tilde{R} , satisfying

$$(1.20) \quad \tilde{R}_{im}^{(-1)} \gamma_{mn}^{(0)} \tilde{R}_{nj} = \lambda_i \delta_{ij},$$

where

$$(1.21) \quad \tilde{R} = RD, \quad D = \text{diag}(d_1, \dots, d_n)$$

with non vanishing d_1, \dots, d_n . Since the eigenvalues of $\gamma_{ij}^{(0)}$ are all real and distinct it can be shown that it is always possible to choose the diagonal matrix D in such a way that \tilde{R} is an orthogonal matrix. Let us then use R such that it is an orthogonal matrix, this in turn means that:

$$(1.22) \quad R_{im} R_{mj}^{(-1)} = \delta_{ij} \quad \text{where} \quad \det R = 1.$$

Once this has been done, the solution can be written as

$$(1.23) \quad f_i(N, \tau) = R_{im} U_{mn}(N, 0, \tau) R_{nj} f_j(N, 0),$$

and the LO form of the matrix U reads

$$(1.24) \quad U_{ij}(N, 0, \tau) = \left(\frac{\alpha_S(0)}{\alpha_S(\tau)} \right)^{\lambda_j(N)/2\pi b_0} \delta_{ij}.$$

Then defining Γ , inverting eq. (1.24), expanding in power of α_S and substituting τ :

$$(1.25) \quad \begin{aligned} \Gamma_{ij}^{(n_f)}(N, \mu_0^2, \mu^2) &= R_{im} U_{mn}^{(n_f)}(N, \mu^2, \mu_0^2) R_{nj} \\ &= \delta_{ij} + \frac{\alpha_S^{(n_f)}(\mu_0^2)}{2\pi} \log \frac{\mu^2}{\mu_0^2} \gamma_{ji}^{(n_f), (0)} + \frac{\alpha_S^2(\mu_0^2)}{8\pi^2} \log^2 \frac{\mu^2}{\mu_0^2} \left(\gamma_{jk}^{(0)} \gamma_{ki}^{(0)} - 6\pi b_0 \gamma_{ji}^{(n_f), (0)} \right) \end{aligned}$$

This is the $O(\alpha_S^2)$ LO solution of the DGLAP equations for the evolution kernel in Mellin space.

1.3 The NLO solution of the DGLAP equations

We will also need the two loop solution of the DGLAP equations, expressed in power of α_S .

At NLO, eq. (1.18) reads

$$(1.26) \quad \frac{df_i(N, \tau)}{d\tau} = \gamma_{ij}^{(0)}(N) f_j(N, \tau) + \frac{\alpha_S(\tau)}{2\pi} \gamma_{ij}^{(1)}(N) f_j(N, \tau) + \dots$$

Let us also call

$$(1.27) \quad \hat{\gamma}_{ij}^{(1)} = R_{im}^{-1} \gamma_{mn}^{(1)} R_{nj},$$

where the matrix R was defined in eq. (1.22). Then, the NLO form of the matrix U is, dropping the N dependence,

$$(1.28) \quad U_{ij}(\mu_0^2, \mu^2) = \left(\frac{\alpha_S(\mu_0^2)}{\alpha_S(\mu^2)} \right)^{\lambda_i/2\pi b_0} \delta_{ij} + \frac{\hat{\gamma}_{ij}^{(1)} - b_1 \lambda_i \delta_{ij}}{\lambda_i - \lambda_j + 2\pi b_0} \left[\alpha_S(\mu_0^2) \left(\frac{\alpha_S(\mu_0^2)}{\alpha_S(\mu^2)} \right)^{\lambda_i/2\pi b_0} - \alpha_S(\mu^2) \left(\frac{\alpha_S(\mu_0^2)}{\alpha_S(\mu^2)} \right)^{\lambda_j/2\pi b_0} \right]$$

Now, using eq. (1.7), one obtains, up to $O(\alpha_S^3)$:

$$(1.29) \quad U_{ij}(\mu_0^2, \mu^2) = \delta_{ij} + \frac{\alpha_S(\mu^2)}{2\pi} \log \frac{\mu^2}{\mu_0^2} \lambda_i \delta_{ij} + \frac{\alpha_S^2(\mu^2)}{4\pi} \log \frac{\mu^2}{\mu_0^2} \left(2\hat{\gamma}_{ij}^{(1)} + \log \frac{\mu^2}{\mu_0^2} \lambda_i \left(\frac{\lambda_i}{2\pi} - b_0 \right) \delta_{ij} \right)$$

which, inverting eq. (1.29), gives:

$$(1.30) \quad \Gamma_{ij}(\mu_0^2, \mu^2) = \delta_{ji} + \frac{\alpha_S(\mu^2)}{2\pi} \log \frac{\mu^2}{\mu_0^2} \gamma_{ji}^{(0)} + \frac{\alpha_S^2(\mu^2)}{4\pi} \log \frac{\mu^2}{\mu_0^2} \left(2\gamma_{ji}^{(1)} + \frac{1}{2\pi} \log \frac{\mu^2}{\mu_0^2} \gamma_{jk}^{(0)} \gamma_{ki}^{(0)} - b_0 \log \frac{\mu^2}{\mu_0^2} \gamma_{ji}^{(0)} \right) + O(\alpha_S^3).$$

Finally we can then define

$$(1.31) \quad \Gamma_{ij}^{(n_f), (1)}(\mu_0^2, \mu^2) = \frac{1}{2\pi} \log \frac{\mu^2}{\mu_0^2} \gamma_{ji}^{(n_f), (0)} \\ \Gamma_{ij}^{(n_f), (2)}(\mu_0^2, \mu^2) = \frac{1}{4\pi} \log \frac{\mu^2}{\mu_0^2} \left(2\gamma_{ji}^{(n_f), (1)} + \frac{1}{2\pi} \log \frac{\mu^2}{\mu_0^2} \gamma_{jk}^{(n_f), (0)} \gamma_{ki}^{(n_f), (0)} - b_0 \log \frac{\mu^2}{\mu_0^2} \gamma_{ji}^{(n_f), (0)} \right)$$

in order to write:

$$(1.32) \quad \Gamma_{ij}^{(n_f)}(\mu_0^2, \mu^2) = \delta_{ij} + \alpha_S^{(n_f)}(\mu^2) \Gamma_{ij}^{(n_f), (1)}(\mu_0^2, \mu^2) + \left(\alpha_S^{(n_f)}(\mu^2) \right)^2 \Gamma_{ij}^{(n_f), (2)}(\mu_0^2, \mu^2).$$

Chapter 2

Comparing the 4F and the 5F scheme

We already saw that calculations of high energy processes involving bottom quarks are typically performed in two different ways. One option, the *massive* or 4F scheme, consists in not including bottom and top quarks among partons. This means that one assumes them not to contribute to the β function and to the anomalous dimensions, *i.e.* to decouple. This is an effective theory with n_f active light quark where the heavy quark are decoupled. Hence, for this approach to be reliable, the heavy quark mass must be of the same order as that of the other hard scales involved.

Alternatively, one may face the situation where the typical scale of the process Q is way higher than the heavy quark mass and logarithms of the type $\log Q^2/m_b^2$ (initial or final state ones) appear that might spoil the convergence of a fixed-order perturbative expansion. In this case, one considers a scheme in which the heavy quark mass is treated as a small parameter, power corrections of the ratio m_b^2/Q^2 are pushed to higher orders and towers of $\log^m Q^2/m_b^2$ are explicitly re-summed via the Altarelli-Parisi equations into a b -PDF. This scheme is referred to the *massless* or 5F scheme.

In the rest of this chapter we will review some analytical properties of this two schemes at NLO. In the final section a numerical comparison for two interesting processes will be presented.

2.1 Analytical comparison between the 4F and the 5F scheme

Recall that in any scheme in perturbative QCD the total cross section (and its differential distribution as well) can be written, for a single scale process, as

(2.1)

$$\sigma^{(n_f)}(s, Q^2) = \sum_{ij}^{n_f} \iint dx_1 dx_2 f_i^{(n_f)}(x_1, \mu_F^2) f_j^{(n_f)}(x_2, \mu_F^2) \hat{\sigma}_{ij}^{(n_f)}(x_1 x_2 s, \mu_F^2, \mu_R^2, Q^2),$$

where $\hat{\sigma}_{ij}$ is the partonic cross section involving initial state partons i, j , which, coming from a hadron, carry a fraction x_p of the p th incoming hadron, μ_F and μ_R are, respectively, the scales at which the factorization and the re-normalization is performed and s is the hadronic center of mass energy, and Q is the hard scale of the process, for instance, in the case of the production of a vector boson V , $Q^2 = M_V^2$. We can now use the Mellin transform defined as

$$(2.2) \quad g(N) = \int_0^{\infty} dx x^{N-1} h(x),$$

where g and h are two generic functions, to write eq. (2.1) in Mellin space

$$(2.3) \quad \sigma^{(n_f)}(Q^2) = \sum_i^{n_f} f_i^{(n_f)}(\mu_F^2) C_i^{(n_f)}(\mu_F^2, \mu_R^2, Q^2),$$

in the case of lepton-hadron scattering, where

$$(2.4) \quad \sigma_{LO}^{(n_f)} C_i^{(n_f)}(N, \mu_F^2, \mu_R^2, Q^2) = \int_0^{\infty} dx x^{N-1} \hat{\sigma}_i^{(n_f)}(x, \mu_F^2, \mu_R^2, Q^2).$$

The C_i s are called the coefficient functions.

The complete functional form of the the factorization and re-normalization scales dependence in the coefficient functions are determined by the running of the coupling α_S and by the evolution of the PDFs. Indeed, we can write eq. (2.3) as follows:

$$(2.5) \quad \sigma^{(n_f)}(Q^2) = \sum_{ij}^{n_f} \left(\alpha_S^{(n_f)}(Q^2) \right)^N \left(C_i^{(0)} + \alpha_S^{(n_f)}(Q^2) C_i^{(1)} + O(\alpha_S^2) \right) \Gamma_{ij}^{(n_f)}(\mu_F^2, Q^2) f_j^{(n_f)}(\mu_F^2).$$

Using eq. (1.25), together with eq. (1.6), one obtains at NLO,

$$(2.6) \quad \sigma^{(n_f)}(Q^2) = \left(\alpha_S^{(n_f)}(\mu_R^2) \right)^N \sum_j^{(n_f)} \left\{ C_j^{(n_f),(0)} - \alpha_S^{(n_f)}(\mu_R^2) \left(N b_0^{(n_f)} \log \frac{Q^2}{\mu_R^2} C_j^{(n_f),(0)} - C_j^{(n_f),(1)} \right) \right. \\ \left. + \sum_i^{(n_f)} \frac{\alpha_S(\mu_R^2)}{2\pi} \log \frac{Q^2}{\mu_F^2} C_i^{(n_f),(0)} \gamma_{ji}^{(n_f),(0)} \right\} f_j^{(n_f)}(\mu_F^2) + O(\alpha_S^{N+2})$$

This formula is easily generalized to hadron-hadron scattering processes, in

which it is:

$$(2.7) \quad \sigma^{(n_f)}(Q^2) = \left(\alpha_S^{(n_f)}(\mu_R^2) \right)^N \sum_{ij}^{n_f} \left\{ C_{ij}^{(n_f),(0)} + \alpha_S^{(n_f)}(\mu_R^2) \left(C_{ij}^{(n_f),(1)} - N b_0^{(n_f)} \log \frac{Q^2}{\mu_R^2} C_{ij}^{(n_f),(0)} \right) \right. \\ \left. + \frac{\alpha_S^{(n_f)}(\mu_R^2)}{2\pi} \sum_{mn}^{(n_f)} C_{mn}^{(n_f),(0)} \log \frac{Q^2}{\mu_F^2} \left(\gamma_{jn}^{(n_f),(0)} \delta_{im} + \gamma_{im}^{(n_f),(0)} \delta_{jn} \right) \right\} f_i^{(n_f)}(\mu_F^2) f_j^{(n_f)}(\mu_F^2)$$

Note that there is an implicit Q^2 dependence, in the previous two equations, through n_f , since, in fact, in the 5F scheme

$$(2.8) \quad n_f(Q^2) \equiv \begin{cases} 3 & \text{if } Q^2 < m_c^2 \\ 4 & \text{if } Q^2 < m_b^2 \\ 5 & \text{if } Q^2 > m_b^2 \end{cases},$$

whereas in the 4F scheme

$$(2.9) \quad n_f(Q^2) \equiv \begin{cases} 3 & \text{if } Q^2 < m_c^2 \\ 4 & \text{if } Q^2 > m_c^2 \end{cases},$$

where m_c is the mass of the charm quark. It has also to be noted that here and in the rest, we assumed that there is only one physical scale, Q^2 , so that the C_i s must be scale independent. If more than one physical scale is present, C would also depend on them. Assume for example that there is another physical scale such as the transverse momentum of a hard probe, p_T . Then C must also be a function of p_T but only through dimensionless ratio p_T^2/Q^2 . Where more than a physical scale is present (once one have chosen the reference scale), results obtained in the rest of this work are still valid but have to be considered as functions of these scales. However, in such cases, one could also choose p_T as a hard scale and then view the whole argument presented with p_T instead of Q . Which of the various choice one can adopt as a hard scale is the best depends on physical arguments.

We can now check that the 4F and the 5F scheme are indeed equal up to higher order corrections and up to m^2/Q^2 corrections. We do this noting that the dependence on n_f only appears in the value of the anomalous dimensions, in the running of the coupling and in the number of values the summation-index can take. We can then get rid of it choosing $\mu_F = \mu_R = m_b$. In this case using again

eq. (1.25) and eq. (1.6),

(2.10)

$$\begin{aligned} \sigma^{(n_f)}(Q^2, \mu_R^2, \mu_F^2) &= \alpha_S^N(m_b) \sum_i^{n_f} \left\{ C_i^{(0)} + \alpha_S(m_b^2) \left[-N b_0^{(n_f)} \log \frac{Q^2}{m_b^2} C_i^{(0)} + C_i^{(1)} \right. \right. \\ &\quad \left. \left. + \frac{1}{2\pi} \gamma_{ij}^{(0)} \log \frac{Q^2}{m_b^2} C_j^{(0)} + O(\alpha_S^2) \right] \right\} f_i(m_b^2) \\ &= \sigma^{(n_f)}(Q^2, m_b^2, m_b^2) + O(\alpha_S^{N+2}). \end{aligned}$$

We can now make use of the fact that at the bottom mass, since $n_f(m_b) = 4$, in each schemes the value of the coupling, of the PDFs and that of the coefficient functions are equal, this means that

$$(2.11) \quad \alpha_S^{(4)}(m_b^2) = \alpha_S^{(5)}(m_b^2) + O(\alpha_S^2),$$

$$(2.12) \quad f_i^{(4)}(m_b) = f_i^{(5)}(m_b) + O(\alpha_S^2)$$

and

$$(2.13) \quad C_i^{(p),(4)} = C_i^{(p),(5)} + O(m_b^2/Q^2).$$

Then one obtains

$$(2.14) \quad \sigma^{(4)}(Q^2, m_b^2, m_b^2) = \sigma^{(5)}(Q^2, m_b^2, m_b^2) + O(\alpha_S^{N+2}) + O(m_b^2/Q^2)$$

which in turn, using eq. (2.10), yields

$$(2.15) \quad \sigma^{(4)}(Q^2, \mu_R^2, \mu_F^2) = \sigma^{(5)}(Q^2, \mu_R^2, \mu_F^2) + O(\alpha_S^{N+2}) + O(m_b^2/Q^2)$$

In the 5F scheme, when $Q^2 > m_b^2$, there is a contribution from the evolution of the b -PDF. This term is proportional to $\log Q^2/m_b^2 \gamma_{gq} f_g(m_b^2)$. In the 4F scheme, this term, exactly matches the term arising from a bottom real emission which is also proportional (see eq. 2.6) to $\log Q^2/m_b^2 \gamma_{gq} f_g(m_b^2)$ but with an opposite sign. Note that instead the μ_R -dependent term in eq. (2.6) cancels out because the value of n_f in the running of the coupling matches that of the n_f in the b_0 term in each scheme.

2.2 Some interesting processes

Many interesting processes at the LHC are the Higgs background processes. As a reference, in this thesis we will consider two such processes: $pp \rightarrow W b \bar{b}$ where $W = W^\pm$ and $pp \rightarrow Z b \bar{b}$.

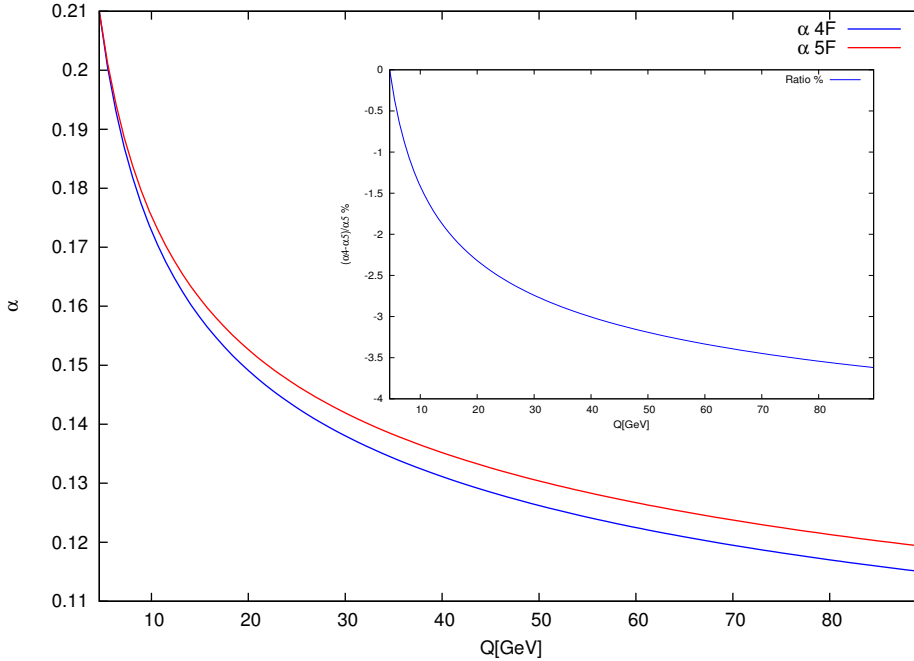


Figure 2.1: The different running of $\alpha_S(Q^2)$ in the 4F(blue) and in the 5F(red) scheme (the large figure) and the ratio between the two (small figure). Note that here we assume that in the schemes the value of the coupling coincides at the bottom mass.

In the following we will present some numerical NLO results for these two processes in the 4F and in the 5F scheme. We briefly report the set-up used for the numerical simulations. The numerical simulations presented here, has been performed in the, fully automated, SHERPA+OPENLOOPS framework [25][18][16].

Whenever we use a non-zero bottom mass, it is fixed at the value $m_b = 4.62$ GeV. The W and Z boson are always considered on-shell with mass $M_W = 80.41$ GeV and $M_Z = 91.1876$ GeV respectively and width $\Gamma_{W,Z} = 0$. The mass of the top quark, which enters in virtual corrections, is set to $m_t = 172.6$ GeV. We use the NLO fixed flavor number scheme NNPDF set of PDFs [7], with $\alpha_S(M_Z) = 0.118$. The Cabibbo-Kobayashi-Maskawa (CKM) matrix is considered to be a unit matrix, hence $V_{du} = V_{cs} = V_{tb} = 1$. This is acceptable because the CKM matrix differ slightly from a unit matrix and we checked that the error due to this choice is relatively small compared to that of the Monte-Carlo integration.

QCD partons in the final state, including b -quarks and excluding only top quarks are recombined into IR-safe jets using the anti- k_T algorithm [14] with jet-resolution parameter $R = 0.7$. We require all events to have a $b\bar{b}$ jet pair in the final state with a transverse momentum (p_T) larger than 25 GeV ($p_T > 25$ GeV) while

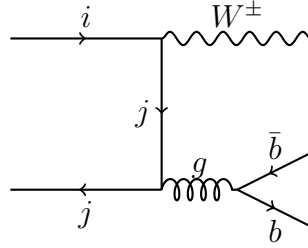


Figure 2.2: Diagram contributing to $pp \rightarrow Wb\bar{b}$.

we do not impose any rapidity or pseudo-rapidity cuts. In this respect we classify as b -jet any jet involving at least a b quark. We also do not impose any cuts on the extra-jet arising due to a hard, non-collinear, real emission of a parton. This hard, non collinear, emission is treated inclusively. This means that we consider both two- and three- jets events at NLO. Finally, the re-normalization and the factorization scale are choose to be $\mu_R = \mu_F = M_V + 2m_b$ where V is the mass of the vector boson ($V = W, Z$).

This processes have been known at NLO for a long time now, both in the massless and in the massive scheme and a full calculation can be found in [21]) while a detailed numerical study is presented in [22].

2.3 $Wb\bar{b}$ production at LHC

The study of W boson production in association with two b jets at the LHC presents many theoretical and experimental facets. On the experimental side, this process is background to $WH(b\bar{b})$ with the Higgs boson decaying to b quarks, to single top and top-pair production and to many new physics searches. On the theoretical side, since it involves heavy quarks, it gives us a testing ground for various calculation techniques.

In fig. (2.1) we show the running of the coupling $\alpha_S(Q^2)$ in the 4F and in the 5F scheme assuming that the value of the two couplings is matched at $Q^2 = m_b^2$, then assuming $\alpha_S^{(5)}(M_Z^2) = 0.118$. Henceforth we will refer to this value of the coupling as the correct value of α_S . We can see from fig. (2.1) that at scales of the order of the mass of the W and the Z bosons the difference between the value of the coupling is around 3%, this means that for processes starting, for example, at $O(\alpha_S^2)$ (as this case is) the difference on the LO cross section in the two schemes is around 12% which is significant. Also note that this difference is increased as the LO order for a considered process has a higher power of α_S .

At LO this process proceeds through the Feynman diagram shown in fig. (2.2). From a LO study, finite bottom mass effects are expected to affect both total and

differential cross section only in the region of small $b\bar{b}$ -pair invariant masses. For this reason, and for that related to the value of α_S , one would be lead to use the 5F scheme in this calculation. However, given the variety of experimental analyses involved for the signal of which $Wb\bar{b}$ is a background, it should be important to precisely access the impact of a finite bottom mass over the entire kinematic reach of the process. This would suggest one to use a massive scheme (as the 4F) to account for this contributions as well.

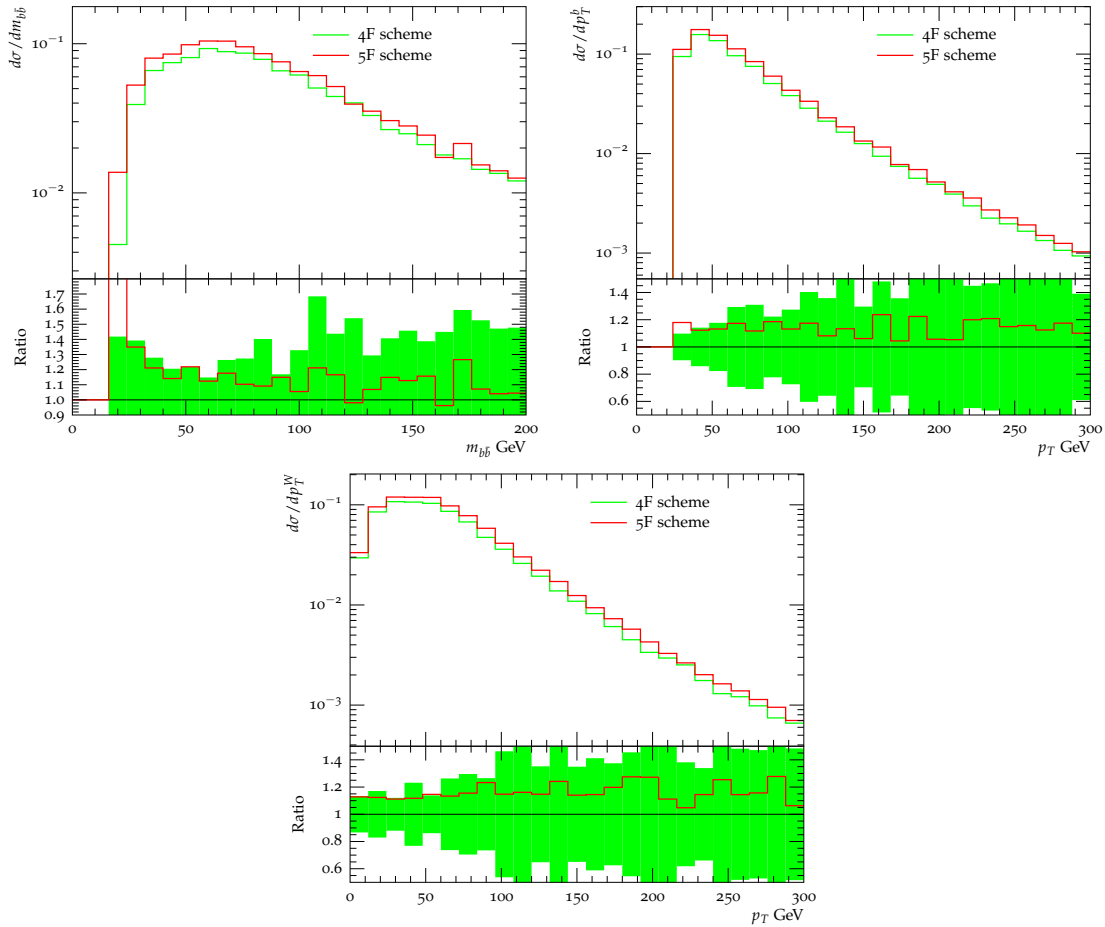


Figure 2.3: Differential distributions for $Wb\bar{b}$ production with respect to the p_T of the W boson(bottom), of the leading p_T jet (top right) or of the invariant mass of the b -jet pair (top left), in the 4F(green) and the 5F(red) scheme. The uncertainty band is that of the Monte-Carlo integration.

In fig. (2.3) we plot the $m_{b\bar{b}}$, p_T^b and p_T^W distribution computed at $\sqrt{s} = 7$ TeV while total the total cross section is reported in tab. (4.1). Here $m_{b\bar{b}}$ is the invariant

mass of the $b\bar{b}$ pair, p_T^b is the transverse momentum of the leading b -jet and p_T^W is the transverse momentum of the W boson. As it can be seen the 4F and the 5F scheme are in reasonable agreement, with differences within 20%. The main difference between the two scheme is in the region of small invariant mass of the $b\bar{b}$ pair, $m_{b\bar{b}} \in [0, 25]$ GeV. In this region, in fact, mass dependent corrections are large. It is easy to see that this must be the case because the cross section in the 5F scheme diverges as $m_{b\bar{b}} \rightarrow 0$ due to a collinear singularity, which is regulated in the 4F scheme by the bottom mass. For this reason $m_b/m_{b\bar{b}}$ correction in this region are large.

Table 2.1: NLO total cross sections for $Wb\bar{b}$ at $\sqrt{s} = 7$ TeV. Each scheme is computed at $\mu_R = \mu_F = M_W + 2m_b$. The error shown is that of the Monte-Carlo integration.

NLO	
$\sigma^{(4F)}$	$\sigma^{(5F)}$
14.8241 pb $\pm 0.28\%$	16.9878 pb $\pm 0.43\%$

2.4 $Zb\bar{b}$ production at LHC

This process also starts at $O(\alpha_S^2)$ and has a massive final state with Q^2 of the order of the mass of the Z boson.

The main difference between W and Z production is that Z production also receives a contribution from the gluon channel. Feynman diagrams for this process are shown in fig. (2.4). The gluon contribution turns out to be dominant and it amounts to 80% of the total cross section. This is because the gluon PDF is much larger than that of other partons.

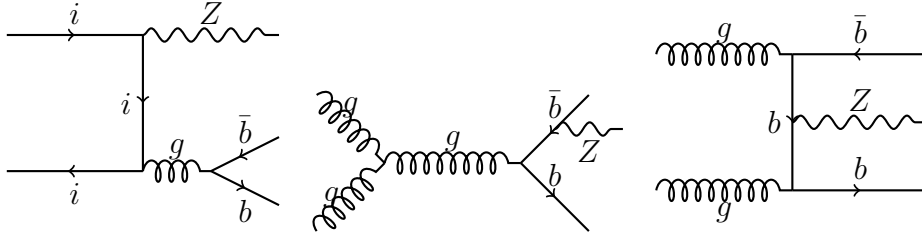


Figure 2.4: Diagrams contributing to $pp \rightarrow Zb\bar{b}$.

Table 2.2: NLO total cross sections for $Zb\bar{b}$ at $\sqrt{s} = 7$ TeV. Each scheme is computed at $\mu_R = \mu_F = M_Z + 2m_b$. The error shown is that of the Monte-Carlo integration.

NLO	
$\sigma^{(4F)}$	$\sigma^{(5F)}$
21.1719 pb $\pm 0.34\%$	24.2749 pb $\pm 0.38\%$

In fig. (2.5) differential distributions for $Zb\bar{b}$ production are shown, again with respect to: the invariant mass of the b -pair ($m_{b\bar{b}}$), the leading b -jet transverse momentum (p_T^b) and the Z boson transverse momentum (p_T^Z); in fig. (4.3) results for

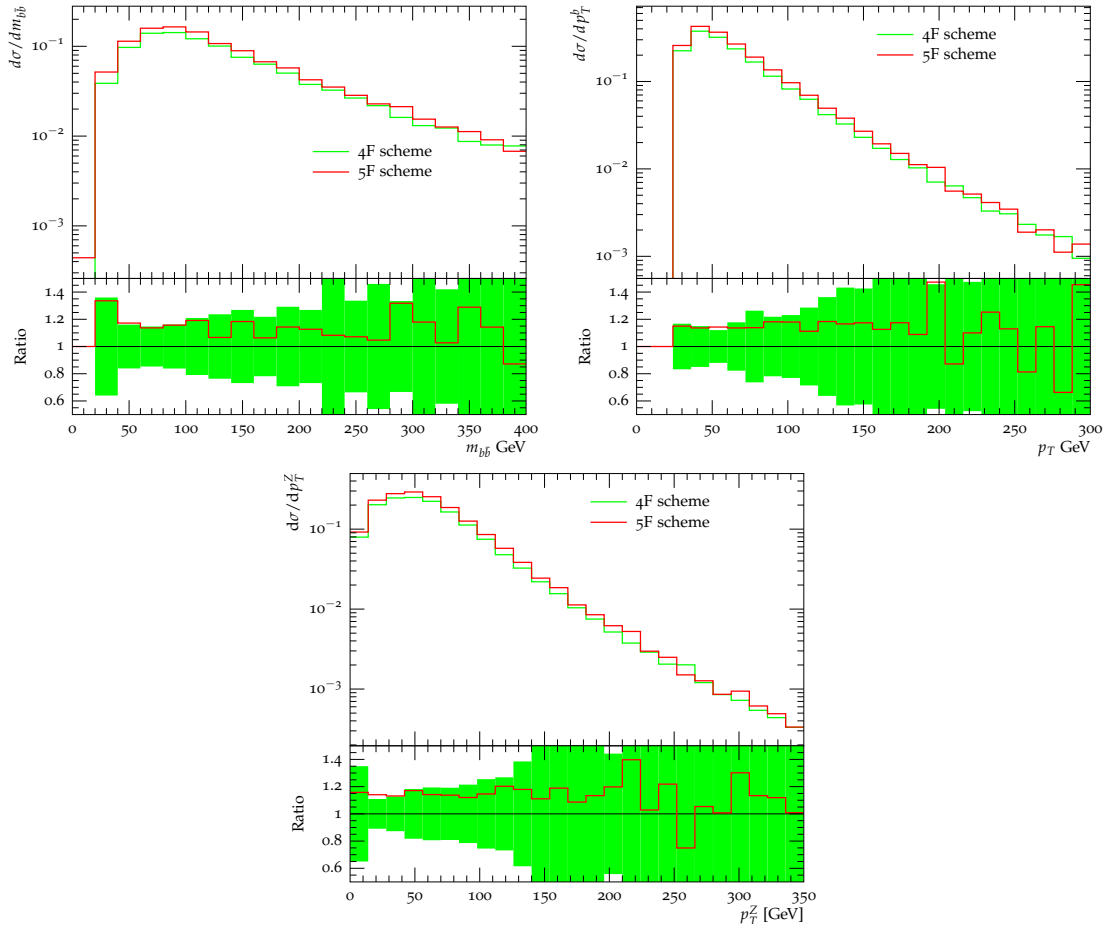


Figure 2.5: Same as fig. (2.3 but for $Zb\bar{b}$ production.

the total cross section in the 4F and in the 5F scheme are shown. Because only the quark channel is affected by a collinear singularity, but not the dominant gluon channel, the agreement between the 4F and the 5F scheme is now better also in the small $m_{b\bar{b}}$ region. Furthermore, in the quark channel, there is a b -initiated contribution which is present in the 5F scheme, but not in the 4F scheme. However 4F and 5F scheme are in good reasonable agreement, both on differential distributions and on total cross section. This suggests that the b -initiated contributions can be negligible. This in turn seems reasonable since they are suppressed by the small value of the b -PDF.

Chapter 3

The doped scheme

In this chapter we present our main result, namely a *doped* scheme.

We define a *doped* scheme: as a scheme obtained by setting $n_f = 4$ everywhere in eq. (2.1), except in the evolution of the running coupling constant, i.e. in eq. (1.5), where we use $n_f = 5$. The rationale for this is that there can be processes in which contributions from the re-summation of initial state logarithms may be negligible with respect to mass suppressed terms (which would suggest to use a massive scheme), but which proceed at such large energy at which the error made using the value of the coupling in a massive scheme can be large.

This means that the factorized cross section translates, in this scheme, in

$$(3.1) \quad \sigma^{(d4)}(s, Q^2) = \sum_{ij}^4 \iint dx_1 dx_2 f_i^{(d)}(x_1, \mu_F^2) f_j^{(d)}(x_2, \mu_F^2) \hat{\sigma}_{ij}^{(d4)}(x_1 x_2 s, \mu_F^2, \mu_R^2, Q^2)$$

with $f_i^{(d)}$ being the solutions of:

$$(3.2) \quad \frac{\partial f_i^{(d)}(x, \mu_F^2)}{\partial \log \mu_F^2} = \sum_j^4 \frac{\alpha_S^{(5)}(\mu_F^2)}{2\pi} P_{ij}^{(4)} \otimes f_j^{(d)}(\mu_F^2)$$

and

$$(3.3) \quad \frac{d\alpha_S^{(5)}(\mu_R^2)}{d \log \mu_R^2} = \beta^{(5)}(\alpha_S) = -b_0^{(5)} \left(\alpha_S^{(5)} \right)^2 + \dots$$

and

$$(3.4) \quad \hat{\sigma}_{ij}^{(d4)} = \left(\alpha_S^{(5)} \right)^N \left(\hat{\sigma}_{ij}^{(4),(0)} + \alpha_S^{(5)} \hat{\sigma}_{ij}^{(4),(1)} + O(\alpha_S^2) \right)$$

Note that we did not use the apex (d) on the cross section ((d) as *doped*) but we used $(d4)$. This is due to the fact that the coefficient functions in the scheme so

defined are not yet that of the *doped* scheme we want to propose, and which will be derived in the next section.

It is also interesting to note that such hybrid schemes are already used to include mass suppressed terms, for example the BMSN scheme (see for a review [26]). This method, however, differ from ours in the way PDF evolution is performed. In fact they evolve PDFs in a full 4F scheme, using also $\alpha_S^{(4)}$, whereas we use $\alpha_S^{(5)}$, while they use $\alpha_S^{(5)}$ only in the partonic cross section expansion. Note also that this scheme has been only be applied to Deeply Inelastic Scattering (DIS).

3.1 The *doped* PDF set

In this section we study some properties of the *doped* PDF set, as defined by eq. (3.2).

We start again with the DGLAP equations eqs.(1.12). Recalling the anomalous dimensions γ do depend on the number of active light flavor n_f , in the *doped* scheme, the DGLAP equations have the form

$$(3.5) \quad \frac{df_i^{(d)}(N, \tau^{(5)})}{d\tau^{(5)}} = \gamma_{ij}^{(4)}(N, \tau^{(5)}) f_j^{(d)}(N, \tau^{(5)}),$$

where the n_f dependence is given by:

$$(3.6) \quad \tau^{(n_f)} = \frac{1}{2\pi} \int_{t_0}^t dt' \alpha_S^{(n_f)}(t'), \quad \frac{d\alpha_S^{(n_f)}(\tau)}{d\tau} = -b_0^{(n_f)} \alpha_S (1 + b_1^{(n_f)} \alpha_S + \dots)$$

$$(3.7) \quad \gamma_{ij}^{(n_f)}(N, \tau^{(n_f)}) = \gamma_{ij}^{(0),(n_f)}(N) + \alpha_S^{(n_f)}(\tau) \gamma_{ij}^{(1),(n_f)}(N) + \dots$$

We can then use eq. (1.25) and eq. (1.30) and get

$$(3.8) \quad \begin{aligned} \Gamma_{ij}^{(d)}(\mu_0^2, \mu^2) &= \delta_{ji} + \frac{\alpha_S^{(5)}(\mu^2)}{2\pi} \log \frac{\mu^2}{\mu_0^2} \gamma_{ji}^{(4),(0)} \\ &+ \frac{\left(\alpha_S^{(5)}(\mu^2)\right)^2}{4\pi} \log \frac{\mu^2}{\mu_0^2} \left(2\gamma_{ji}^{(4),(1)} + \frac{1}{2\pi} \log \frac{\mu^2}{\mu_0^2} \gamma_{jk}^{(4),(0)} \gamma_{ki}^{(4),(0)} - b_0^{(5)} \log \frac{\mu^2}{\mu_0^2} \gamma_{ji}^{(4),(0)} \right) + O(\alpha_S^3). \end{aligned}$$

As it was already pointed out by Martin *et al.* in [31], this evolution produces an inconsistency on physical observables. To better understand this point consider for example the gluon contribution to the longitudinal structure function in DIS, F_L . At LO, in the doped scheme, this is

$$(3.9) \quad F_L(x, Q^2) = \alpha_S^{(5)}(Q^2) \left(C_{Lg}^{(1)} \otimes g^{(d)} \right) (x, Q^2)$$

and therefore (dropping the x, Q^2 dependence):

$$(3.10) \quad \frac{\partial F_L}{\partial \log Q^2} = -b_0^{(5)} \alpha_S^2 C_{Lg}^{(1)} \otimes g^{(d)} + \frac{\alpha_S^2}{2\pi} C_{Lg}^{(1)} \otimes p_{gg}^{(4)} \otimes g^{(d)} + \text{quark terms}$$

Since the $p_{gg}^{(n_f)}$ contains a term proportional to $b_0^{(n_f)} \delta(1-z)$ (*i.e.* the gluon loses momentum to the quarks it radiates) it is easy to see that this quantity has a n_f residual dependence which it shouldn't have. In fact when, for example, going from the 4F to the 5F scheme, both n_f changes equally and cancel out, leaving this quantity independent of n_f . In our case this happens because the $O(\alpha_S)$ term in eq. (3.8) is proportional to $\gamma_{gg}^{(4),(0)}$ which in turn has a term proportional to $b_0^{(4)}$, this term, in a hybrid scheme, will no longer match the b_0 proportional term coming from the running of the coupling (which in this case is proportional to $b_0^{(5)}$).

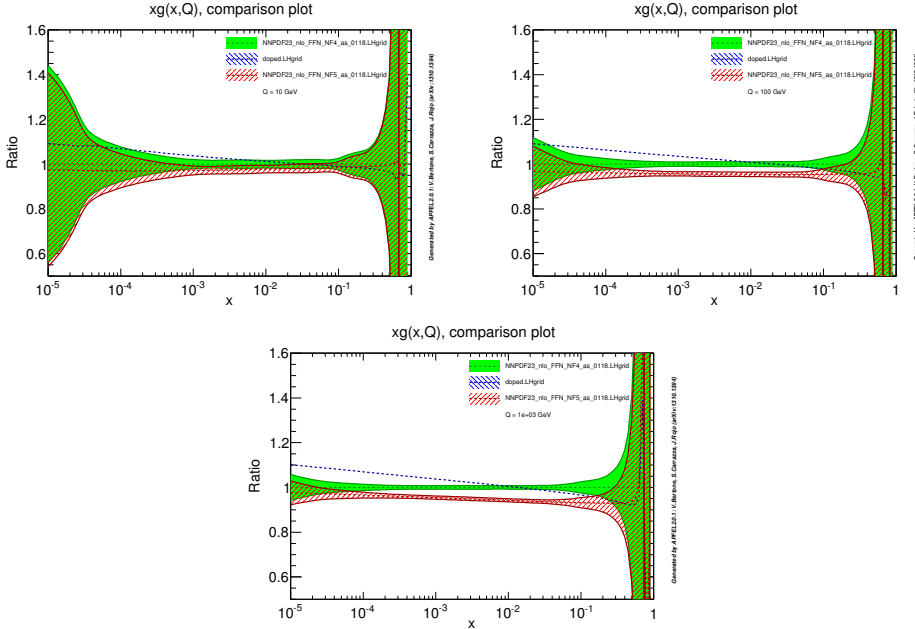


Figure 3.1: Ratio of the gluon density in the 5F (red) and in the doped (black) scheme at $Q^2 = 10, 10^2$ and 10^3 GeV² with respect to the 4F scheme (green).

In fig. (3.1) we show the ratio between the 5F scheme and the 4F scheme and between the doped scheme with the 4F scheme for the gluon PDF. The doped PDF have been obtained [10] by evolving to the bottom mass a standard 4F scheme PDF set, and then using the evolution kernels in eq. (3.8). It is clear from this plot that the differences between the 4F scheme and the doped scheme set are as large as that between the 4F scheme and the 5F scheme.

3.2 Some analytical properties of the doped scheme

We have seen in sect. (2.1) that the 4F and the 5F scheme, provide equivalent results at the level of physical observables. This is the case even if the two schemes are indeed different. In fact the coefficient functions in the 4F scheme are defined as to consistently match, order by order in perturbation theory, terms arising in the 5F scheme from the bottom quark. This means that it must be possible to also construct an equivalent scheme provided only a consistent re-definition of the coefficient functions used in eq. (3.1). In this section we will do that for the doped scheme defined by eq. (3.1). To do this, we use the same trick used in sect. (2.1), namely we choose $\mu_R = \mu_F = m_b$. We will then show that however, if we use the 4F expression for the coefficient function in the doped scheme, the cross section is no longer independent of the re-normalization scale. We can then define

$$(3.11) \quad \sigma^{(d)}(Q^2, \mu_R^2, \mu_F^2) = \sigma^{(d4)}(Q^2, m_b^2, m_b^2) - X(\mu_R^2, \mu_F^2).$$

where $\sigma^{(d)}$ will be the correct expression of the cross section in the doped scheme and X is the residual scale dependent term of $\sigma^{(d4)}$.

To compute $X(\mu_R^2, \mu_F^2)$ we use eqs(3.2) and (1.6). Then

$$(3.12) \quad \sigma^{(d4)}(Q^2, \mu_R^2, \mu_F^2) = \left(\alpha_S^{(5)}(\mu_R^2) \right)^N \sum_i^4 \left\{ C_i^{(4),(0)} + \alpha_S^{(5)}(\mu_R^2) \left[-N b_0^{(4)} \log \frac{Q^2}{\mu_R^2} C_i^{(4),(0)} + C_i^{(4),(1)} + \frac{1}{2\pi} \gamma_{ij}^{(4),(0)} \log \frac{Q^2}{\mu_F^2} C_j^{(4),(0)} + O(\alpha_S^2) \right] \right\} f_j^{(d)}(\mu_F^2).$$

Making use again of the running of the coupling and of the DGLAP equations in the doped scheme, one obtains that

$$(3.13) \quad X(\mu_R^2, \mu_F^2) = \alpha_S^{N+1}(m_b^2)(b_0^{(5)} - b_0^{(4)})N \log \frac{\mu_R^2}{m_b^2} C_i^{(0)} f_i(\mu_F^2) + O(\alpha_S^{N+2}).$$

This means that the μ_R independence is restored if the doped scheme is defined as

$$(3.14) \quad \sigma^{(d)}(Q^2, \mu_R^2, \mu_F^2) = \sigma^{(d4)}(Q^2, \mu_R^2, \mu_F^2) - X(\mu_R^2, \mu_F^2)$$

With this re-definition of the doped scheme, together with the fact that (this property follows by definition of the doped scheme):

$$(3.15) \quad \sigma^{(d)}(Q^2, m_b^2, m_b^2) = \sigma^{(4F)}(Q^2, m_b^2, m_b^2) + O(\alpha_S^{N+2})$$

one obtains:

$$(3.16) \quad \sigma^{(d)}(Q^2, \mu_R^2, \mu_F^2) = \sigma^{(4F)}(Q^2, \mu_R^2, \mu_F^2) + O(\alpha_S^{N+2}).$$

One then gets a scheme in which mass effects are included, logarithms of the type $\log Q^2/\mu_R^2$, are re-summed in α_S but not in the hard cross section, while logarithms of the type $\log Q^2/\mu_F^2$ are not re-summed.

3.3 Consistency of the doped scheme

As was shown in the previous, the difference between the various schemes (with the doped scheme consistently adjusted at NLO) is at least of order $O(\alpha_S^{N+2})$. Let us then define the following quantities,

$$(3.17) \quad \Delta(5F, 4F, Q^2, \mu_R^2, \mu_F^2, m_b^2) = \sigma^{(5F)}(Q^2, \mu_R^2, \mu_F^2) - \sigma^{(4F)}(Q^2, \mu_R^2, \mu_F^2)$$

and

$$(3.18) \quad \Delta(d, 4F, Q^2, \mu_R^2, \mu_F^2, m_b^2) = \sigma^{(d)}(Q^2, \mu_R^2, \mu_F^2) - \sigma^{(4F)}(Q^2, \mu_R^2, \mu_F^2).$$

Let also $\mu_F = \mu_R = \mu$. We now want to separate mass corrections from logarithmic ones. This can be done noticing that we can write:

$$(3.19) \quad \Delta(5F, 4F, Q^2, \mu^2, m_b^2) = h \left(\frac{m^2}{Q^2} \right) = h^{(0)} + \bar{h}$$

and

$$(3.20) \quad \Delta(d, 4F, Q^2, \mu^2, m_b^2) = g \left(\frac{m^2}{Q^2} \right) = g^{(0)} + \bar{g},$$

where $h^{(0)}$ and $g^{(0)}$ are defined to be the limit for $m_b \rightarrow 0$ of h and g respectively, while \bar{h} and \bar{g} are defined so to be the rest of these limits, namely $\bar{h} = h - h^{(0)}$ and $\bar{g} = g - g^{(0)}$. Since $\Delta(5F, 4F)$ is the difference between the 5 and 4 flavor scheme then, we notice that $h^{(0)}$ contains the logarithms present in the 5F scheme but not in the 4F scheme. Since these logs start being different at $O(\alpha_S^2)$ with respect to the LO,

$$(3.21) \quad h^{(0)} = \alpha_S^{N+2} \left(h_{(0)}^{(0)} + \alpha_S h_{(1)}^{(0)} + O(\alpha_S^2) \right).$$

However, since the coefficient functions in the 4F and in the 5F scheme differ in the way they treat mass suppressed terms, \bar{h} actually start already at LO,

$$(3.22) \quad \bar{h} = \alpha_S^N \left(\bar{h}_{(0)} + \alpha_S \bar{h}_{(1)} + O(\alpha_S^2) + O(m_b^2/Q^2) \right).$$

In the case of $\Delta(d, 4F)$, $g^{(0)}$ contains terms proportional to $\log \mu_R^2/m_b^2$ which, as we have seen, are not re-summed in the hard cross section, while $g^{(1)}$ contains mass suppressed terms. However now also \bar{g} start at $O(\alpha_S^2)$ because the doped scheme is a massive scheme, and thus terms can only arise as interference with $\log \mu_R^2/m_b^2$ corrections.

$$(3.23) \quad g^{(0)} = \alpha_S^{N+2} \left(g_{(0)}^{(0)} + \alpha_S g_{(1)}^{(0)} + O(\alpha_S^2) \right)$$

and

$$(3.24) \quad \bar{g} = \alpha_S^{N+2} (\bar{g}_{(0)} + \alpha_S \bar{g}_{(1)} + O(\alpha_S^2) + O(m_b^2/Q^2)).$$

Unresummed higher order terms proportional to powers of $\log \mu_R^2/m_b^2$ could in principle be unnaturally large. The doped scheme is thus advantageous if this is not the case, *i.e.* the following conditions are met:

1. The 4F description should be better than 5F one. So collinear logs, arising from the radiation of a b-quark off a gluon should be small compared to the mass suppressed terms \Rightarrow

$$(3.25) \quad |h^{(0)}| < |\bar{h}|.$$

If this condition is not met, the 5F scheme is the most appropriate.

2. The possible logarithmic terms in the doped scheme must not be large compared to those of the 5F scheme.

$$(3.26) \quad |g^{(0)}| \lesssim |h^{(0)}|.$$

If this condition is not met, the extra sub-leading terms induced by the *doping* are large.

3. Mass suppressed terms in the difference between doped and 4 flavor scheme should be ~ 0 since they treat mass dependence in the same way. One, thus, has to make sure that

$$(3.27) \quad |\bar{g}| < |g^{(0)}|.$$

If this condition is not met, interference between mass corrections and sub-leading logarithmic terms are large.

Note that in this analysis we always assumed that there is only one scale of the process, namely Q^2 . When dealing with a multi-scale problem these conditions may be met only for particular choices of the other hard scales or for a particular range of parameters (such as physical cuts).

3.4 The $O(\alpha_S^{N+2})$ terms

We can try to get an analytic handle on the various quantities in eqs.(3.25,3.26,3.27). To this purpose we make use again of the trick used in the previous sections, namely we express any results in terms of PDF and α_S evaluated at the scale $\mu_R = \mu_F = m_b$.

In the following we assume the physically interesting situation in which $Q^2 \gg m_b^2$. Then for a generic choice $\mu_R = \mu_F = \mu$, using eq. (1.6) together with eq. (1.25) the cross section is

$$\begin{aligned}
\sigma^{(n_f)}(Q^2, \mu^2) &= \alpha_S^N(\mu^2) \sum_i^{n_f} \left\{ C_i^{(0)} + \alpha_S(\mu^2) \left[-Nb_0 \log \frac{Q^2}{\mu^2} C_i^{(0)} + C_i^{(1)} + \frac{1}{2\pi} \log \frac{Q^2}{\mu^2} C_j^{(0)} \gamma_{ij}^{(0)} \right] \right\} f_i(\mu^2) \\
&= \alpha_S^N(m_b^2) \left[1 - \alpha_S(m_b^2) Nb_0 \log \frac{\mu^2}{m_b^2} + \alpha_S^2(m_b^2) \frac{b_0^2}{2} \log^2 \frac{\mu^2}{m_b^2} N(N+1) \right] \\
&\times \sum_i^{n_f} \left\{ C_i^{(0)} + \alpha_S(m_b^2) \left[-Nb_0 \log \frac{Q^2}{\mu^2} C_i^{(0)} + C_i^{(1)} + \frac{1}{2\pi} \log \frac{Q^2}{\mu^2} C_j^{(0)} \gamma_{ij}^{(0)} \right] \right. \\
&\quad \left. - \alpha_S^2(m_b^2) b_0 \log \frac{\mu^2}{m_b^2} \left[-Nb_0 \log \frac{Q^2}{\mu^2} C_i^{(0)} + C_i^{(1)} + \frac{1}{2\pi} \log \frac{Q^2}{\mu^2} C_j^{(0)} \gamma_{ij}^{(0)} \right] \right\} \\
(3.28) \quad &\times \left[\delta_{im} + \frac{\alpha_S(m_b^2)}{2\pi} \log \frac{\mu^2}{m_b^2} \gamma_{im}^{(0)} + \frac{\alpha_S^2(m_b^2)}{8\pi^2} \log^2 \frac{\mu^2}{m_b^2} \left(\gamma_{ik}^{(0)} \gamma_{km}^{(0)} - 6\pi b_0 \gamma_{im}^{(0)} \right) \right] f_m(m_b^2)
\end{aligned}$$

This can be written in the general form:

$$(3.29) \quad \sigma^{(n_f)}(Q^2, \mu^2) = \sigma_{NLO}^{(n_f)}(m_b^2) + \alpha_S^{N+2}(m_b^2) \sum_{p=0}^2 \log^p \frac{\mu^2}{m_b^2} \xi^{(p),(n_f)} \left(\frac{Q^2}{m_b^2} \right).$$

We now observe that if $\mu = m_b$ then all schemes coincides. On the other hand, with this choice there are large corrections of order $\log Q^2/\mu^2$. It is thus advantageous to study the accuracy of the doped scheme when one make a natural choice $\mu \sim Q^2$. In this case, logarithms of the type $\log \mu^2/m_b^2$ are potentially large. We then extract the leading correction as the largest coefficient proportional to the lowest order, *i.e.* the term proportional to $\alpha_S^{N+2} \log^2$. Then we can write the previous equation as

$$(3.30) \quad \sigma^{(n_f)}(Q^2, \mu^2) = \sigma_{NLO}^{(n_f)}(m_b^2) + \alpha_S^{N+2}(m_b^2) \log^2 \frac{\mu^2}{m_b^2} \xi^{(2),(n_f)} \left(\frac{Q^2}{m_b^2} \right),$$

with

$$\begin{aligned}
\xi^{(2),(n_f)} \left(\frac{Q^2}{m_b^2} \right) &= - \sum_{j=0}^{n_f} \left\{ \frac{1}{2} \left(b_0^{(n_f)} \right)^2 N(1+N) C_j^{(0)} \right. \\
(3.31) \quad &\quad \left. + \frac{1}{8\pi^2} \sum_{i=0}^{n_f} \left[\sum_{k=0}^{n_f} \gamma_{ki}^{(n_f),(0)} \gamma_{jk}^{(n_f),(0)} + 2\pi b_0^{(4)} (2N-1) \gamma_{ji}^{(n_f),(0)} \right] C_i^{(0)} \right\} f_j(m_b^2)
\end{aligned}$$

Then, using the fact that $\sigma_{NLO}^{(4F)} = \sigma_{NLO}^{(5F)} + O(\alpha_S^{N+2})$ we can write

$$(3.32) \quad \begin{aligned} h^{(0)}(Q^2, \mu^2) &= (\sigma^{(5F)}(Q^2, \mu^2) - \sigma^{(4F)}(Q^2, \mu^2)) \\ &= \log^2 \frac{\mu^2}{m_b^2} \left(\xi^{(2),(5F)} \left(\frac{Q^2}{m_b^2} \right) - \xi^{(2),(4F)} \left(\frac{Q^2}{m_b^2} \right) \right) \end{aligned}$$

and also, of course,

$$(3.33) \quad \begin{aligned} g^{(0)}(Q^2, \mu^2) &= (\sigma^{(d)}(Q^2, \mu^2) - \sigma^{(4F)}(Q^2, \mu^2)) \\ &= \log^2 \frac{\mu^2}{m_b^2} \left(\xi^{(2),(d)} \left(\frac{Q^2}{m_b^2} \right) - \xi^{(2),(4F)} \left(\frac{Q^2}{m_b^2} \right) \right). \end{aligned}$$

In practice what do we need to compute in order to check the three conditions previously defined, is just $\xi^{(2),(5F)} \left(\frac{Q^2}{m_b^2} \right) - \xi^{(2),(4F)} \left(\frac{Q^2}{m_b^2} \right)$ and $\xi^{(2),(d)} \left(\frac{Q^2}{m_b^2} \right) - \xi^{(2),(4F)} \left(\frac{Q^2}{m_b^2} \right)$. Let us write the expression of $\xi^{(2)}$ in the various schemes.

$$(3.34) \quad \begin{aligned} \xi^{(2),(4)} \left(\frac{Q^2}{m_b^2} \right) &= - \sum_{j=0}^4 \left\{ \frac{1}{2} \left(b_0^{(4)} \right)^2 N(1+N) C_j^{(0)} \right. \\ &\quad \left. + \frac{1}{8\pi^2} \sum_{i=0}^4 \left[\sum_{k=0}^4 \gamma_{ki}^{(4),(0)} \gamma_{jk}^{(4),(0)} + 2\pi b_0^{(4)} (2N-1) \gamma_{ji}^{(4),(0)} \right] C_i^{(0)} \right\} f_j(m_b^2), \end{aligned}$$

$$(3.35) \quad \begin{aligned} \xi^{(2),(5)} \left(\frac{Q^2}{m_b^2} \right) &= - \sum_{j=0}^5 \left\{ \frac{1}{2} \left(b_0^{(5)} \right)^2 N(1+N) C_j^{(0)} \right. \\ &\quad \left. + \frac{1}{8\pi^2} \sum_{i=0}^5 \left[\sum_{k=0}^5 \gamma_{ki}^{(5),(0)} \gamma_{jk}^{(5),(0)} + 2\pi b_0^{(5)} (2N-1) \gamma_{ji}^{(5),(0)} \right] C_i^{(0)} \right\} f_j(m_b^2) \end{aligned}$$

and

$$(3.36) \quad \begin{aligned} \xi^{(2),(d)} \left(\frac{Q^2}{m_b^2} \right) &= - \sum_{j=0}^4 \left\{ \frac{1}{2} \left(b_0^{(5)} \right)^2 N(1+N) C_j^{(0)} \right. \\ &\quad \left. + \frac{1}{8\pi^2} \sum_{i=0}^4 \left[\sum_{k=0}^4 \gamma_{ki}^{(4),(0)} \gamma_{jk}^{(4),(0)} + 2\pi b_0^{(5)} (2N-1) \gamma_{ji}^{(4),(0)} \right] C_i^{(0)} \right\} f_j(m_b^2). \end{aligned}$$

Now we can define,

$$(3.37) \quad a_1 = \frac{1}{2} N(N+1) \sum_{j=0}^4 \left(- \left(b_0^{(5)} \right)^2 + \left(b_0^{(4)} \right)^2 \right) C_j^{(0)} f_j(m_b^2),$$

$$(3.38) \quad a_2 = -\frac{1}{8\pi^2} \sum_{ij=0}^4 \left[\sum_{k=0}^4 \left(\gamma_{ki}^{(5),(0)} \gamma_{jk}^{(5),(0)} - \gamma_{ki}^{(4),(0)} \gamma_{jk}^{(4),(0)} \right) + 2\pi (2N-1) \left(b_0^{(5)} \gamma_{ji}^{(5),(0)} - b_0^{(4)} \gamma_{ji}^{(4),(0)} \right) \right] C_i^{(0)} f_j(m_b^2),$$

while we define a_3 to be the contribution, which was not included in the previous terms, of the bottom quark to the 5F scheme. This term is

$$(3.39) \quad a_3 = \frac{1}{8\pi^2} C_b^{(0)} \gamma_{gq}^{(0)} \left(2\gamma_{qq}^{(0)} - 6\pi b_0^{(5)} + \gamma_{gg}^{(0)} \right) f_g(m_b^2).$$

since $f_b(m_b) = 0$. Then

$$(3.40) \quad \xi^{(2),(5F)} \left(\frac{Q^2}{m_b^2} \right) - \xi^{(2),(4F)} \left(\frac{Q^2}{m_b^2} \right) = a_1 + a_2 + a_3.$$

Using $\gamma_{ij}^{(4)} = \gamma_{ij}^{(5)} - 2\pi(b_0^{(5)} - b_0^{(4)})\delta_{ij}$ one gets

$$(3.41) \quad a_1 = -\sum_{j=0}^4 \frac{1}{2} \left(\left(b_0^{(5)} \right)^2 - \left(b_0^{(4)} \right)^2 \right) N(1+N) C_j^{(0)} f_j(m_b^2),$$

$$(3.42) \quad a_2 = \frac{\left(b_0^{(5)} - b_0^{(4)} \right)}{4\pi} \left\{ \left[\left(2\pi b_0^{(5)} - (2N-1)\gamma_{gg}^{(0)} \right) f_g(m_b^2) - (2N-1)\gamma_{qq}^{(0)} \sum_{i=q,\bar{q}} f_i(m_b^2) \right] C_g^{(0)} - \sum_{i=q,\bar{q}} \left[(2N-1)\gamma_{gq}^{(0)} f_g(m_b^2) + (2N-1)\gamma_{qq}^{(0)} f_i(m_b^2) \right] C_i^{(0)} \right\}$$

and

$$(3.43) \quad a_3 = \frac{1}{8\pi^2} C_b^{(0)} \gamma_{gq}^{(0)} \left(2\gamma_{qq}^{(0)} - 6\pi b_0^{(5)} + \gamma_{gg}^{(0)} \right) f_g(m_b^2).$$

In this way the first contribution is that coming from the different value of b_0 in the running of the coupling, the second comes from the different value of b_0 in the gluon-gluon splitting function while the last term is the bottom contribution to the 5F scheme.

repeating the same argument for $g^{(0)}$, one then finds that

$$(3.44) \quad \xi^{(2),(d)} \left(\frac{Q^2}{m_b^2} \right) - \xi^{(2),(4F)} \left(\frac{Q^2}{m_b^2} \right) = d_1 + d_2 + d_3,$$

with

$$(3.45) \quad \begin{aligned} d_1 &= a_1, \\ d_3 &= 0 \end{aligned}$$

and d_2 :

$$(3.46) \quad d_2 = \frac{(b_0^{(5)} - b_0^{(4)})}{4\pi} (1 - 2N) \left\{ C_g^{(0)} \left[\gamma_{gg}^{(0)} f_g(m_b^2) + \gamma_{gq}^{(0)} \sum_{i=q,\bar{q}} f_i(m_b^2) \right] + \sum_{i=q,\bar{q}} C_i^{(0)} \left[\gamma_{qg}^{(0)} f_g(m_b^2) + \gamma_{qq}^{(0)} f_i(m_b^2) \right] \right\}.$$

With this results, the three conditions presented (eqs.(3.25,3.26,3.27)) imply that:

$$(3.47) \quad \begin{aligned} \log^2 \frac{\mu^2}{m_b^2} (a_1 + a_2 + a_3) &< \frac{m_b^2}{Q^2} h^{(1)} \\ a_2 + a_3 &\sim d_2 \\ \log^2 \frac{\mu^2}{m_b^2} (a_1 + d_2) &> \frac{m_b^2}{Q^2} g^{(1)}. \end{aligned}$$

which yield that, for doping to be advantageous one has to make sure that

$$(3.48) \quad \frac{m^2}{Q^2} g^{(1)} \lesssim (a_1 + d_2) \log^2 \frac{\mu^2}{m_b^2} \lesssim \frac{m_b^2}{Q^2} h^{(1)}.$$

Chapter 4

Comparing the doped scheme with the 4F and the 5F scheme

In this chapter we study the phenomenological relevance of the doped scheme, using as examples the processes $W/Zb\bar{b}$ production. Numerical results in this section are obtained using the same experimental settings of sect. (2.2). In order to study the dependence of our results on other physical scales we also report numerical results for a cut on the b -jets of $p_T^{cut} > 5$ GeV.

4.1 $Wb\bar{b}$ production at LHC

Table 4.1: NLO cross sections for $Wb\bar{b}$ at $\sqrt{s} = 7$ TeV. Each scheme is computed at $\mu_R = \mu_F = M_W + 2m_b$. The errors shown are the Monte-Carlo errors.

NLO, $p_T^{cut} > 25$ GeV		
$\sigma^{(4F)}$	$\sigma^{(5F)}$	$\sigma^{(d)}$
14.8241 pb $\pm 0.28\%$	16.9878 pb $\pm 0.43\%$	16.5539 pb $\pm 0.27\%$
NLO, $p_T^{cut} > 5$ GeV		
$\sigma^{(4F)}$	$\sigma^{(5F)}$	$\sigma^{(d)}$
113.823 pb $\pm 0.21\%$	185.044 pb $\pm 0.38\%$	127.211 pb $\pm 0.21\%$

In fig. (4.1) we show differential distributions with respect to the b -pair invariant mass ($m_{b\bar{b}}$) the p_T of the leading b -jet and that of the W boson for p_T of the b -jet

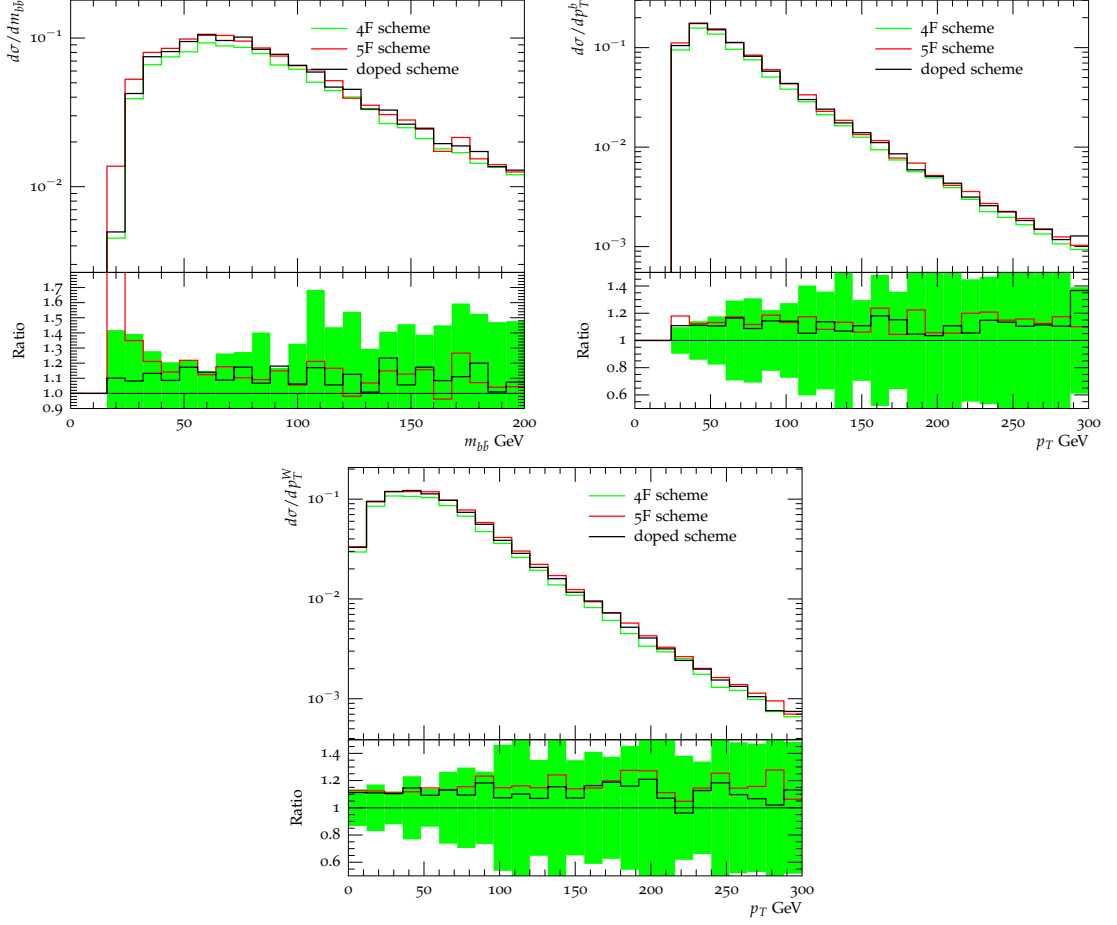


Figure 4.1: Differential distributions for $Wb\bar{b}$ production with respect to the p_T of the W boson (bottom), of the leading p_T jet (top right) or of the invariant mass of the b -jet pair (top left), in the 4F (green), in the 5F (red) and in the doped scheme (black). The uncertainty band is that of the Monte-Carlo integration. Numerical results are obtained with $p_T^{cut} > 25$ GeV.

$p_T^{cut} > 25$ GeV (results for $p_T^{cut} > 5$ GeV are shown in fig. (4.2)), while in tab. (4.1) we report numerical results for the total cross section. As it can be seen from the results for $p_T^{cut} > 25$ GeV, the doped scheme is essentially indistinguishable from the 5F scheme, except at small $m_{b\bar{b}}$, where it agrees with the 4F scheme. This suggests that the dominant difference between the 4F and the 5F scheme, in this case, is the value of α_S , which is correctly reproduced by the doped scheme, except at small $m_{b\bar{b}}$ where the 5F scheme has a collinear singularity which is regulated by the bottom mass in the doped scheme. We therefore expect that at the level

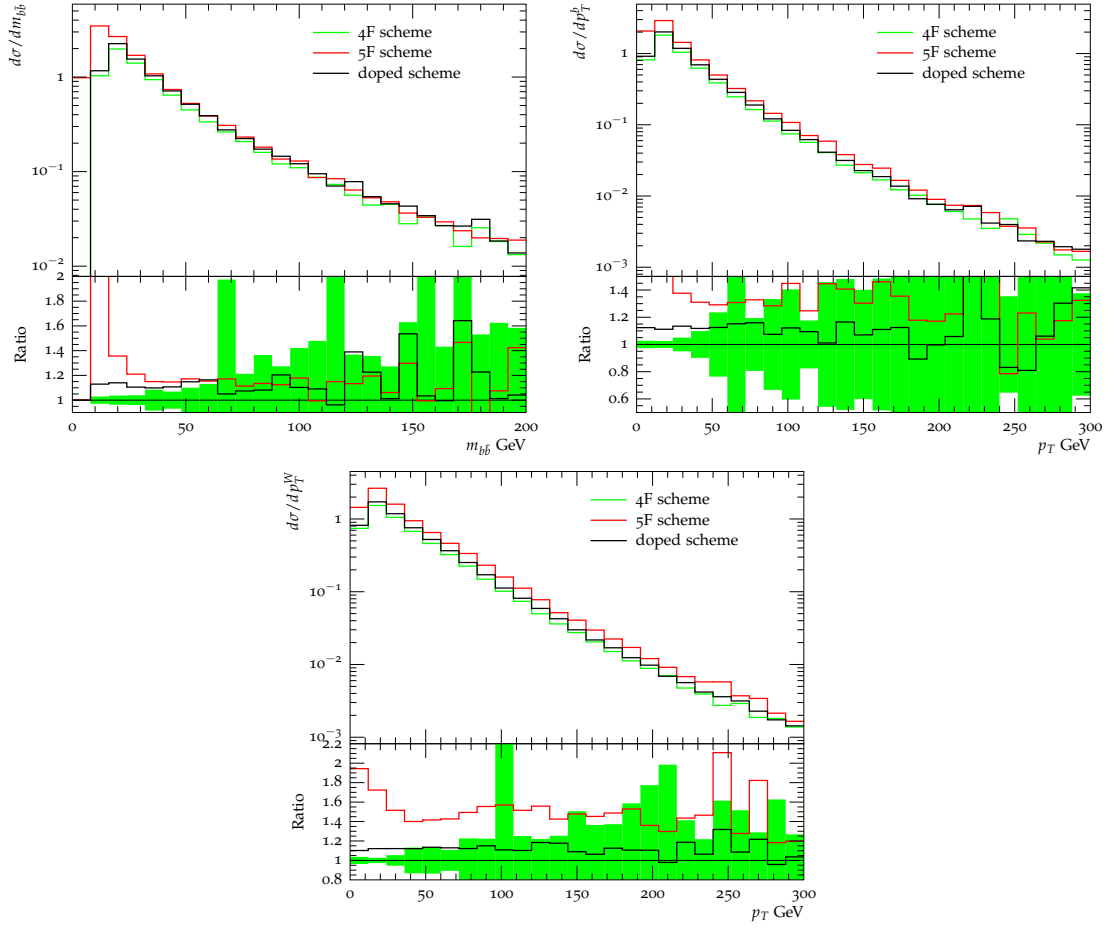


Figure 4.2: Same as fig. (4.1) with $p_T^{cut} > 5$ GeV.

of total cross section the impact of mass corrections is negligible. Indeed we can check this by making use of the conditions defined in the previous chapter, namely eq. (3.25), eq. (3.26) and eq. (3.27).

Recall that we defined,

$$(4.1) \quad \Delta(5F, 4F, Q^2, \mu^2, m_b^2) = h^{(0)} + \bar{h}$$

and

$$(4.2) \quad \Delta(d, 4F, Q^2, \mu^2, m_b^2) = g^{(0)} + \bar{g}$$

then:

$$(4.3) \quad \begin{aligned} h^{(0)} &= \Delta(5F, 4F, Q^2, \mu^2, 0), \\ g^{(0)} &= \Delta(d, 4F, Q^2, \mu^2, 0) \end{aligned}$$

and finally

$$(4.4) \quad \begin{aligned} \bar{h} &= \Delta(5F, 4F, Q^2, \mu^2, m_b^2) - \Delta(5F, 4F, Q^2, \mu^2, 0) \\ \bar{g} &= \Delta(d, 4F, Q^2, \mu^2, m_b^2) - \Delta(d, 4F, Q^2, \mu^2, 0). \end{aligned}$$

The numerical value of eq. (4.3) is reported in tab. (4.2) and the exact way used to obtain it is given in the appendix. Note that in the appendix also an analytical approach to compute the same limit is given, although results obtained using that method are not reported here since they need to be validated. As we expected,

Table 4.2: $h^{(0)}, g^{(0)}, \bar{h}, \bar{g}$ values for $Wb\bar{b}$ production.

$p_T^{cut} > 25 \text{ GeV}$			
$\Delta(5F, 4F, Q^2, \mu^2, m_b^2)$	$\Delta(5F, 4F, Q^2, \mu^2, 0)$	$h^{(0)}$	\bar{h}
2.1634 pb	1.47957 pb	1.47957 pb	0.68383 pb
$p_T^{cut} > 5 \text{ GeV}$			
$\Delta(d, 4F, Q^2, \mu^2, m_b^2)$	$\Delta(d, 4F, Q^2, \mu^2, 0)$	$g^{(0)}$	\bar{g}
1.7298 pb	1.67011 pb	1.67011 pb	0.05969 pb
$p_T^{cut} > 5 \text{ GeV}$			
$\Delta(5F, 4F, Q^2, \mu^2, m_b^2)$	$\Delta(5F, 4F, Q^2, \mu^2, 0)$	$h^{(0)}$	\bar{h}
71.221 pb	15.168 pb	15.168 pb	56.053 pb
$p_T^{cut} > 5 \text{ GeV}$			
$\Delta(d, 4F, Q^2, \mu^2, m_b^2)$	$\Delta(d, 4F, Q^2, \mu^2, 0)$	$g^{(0)}$	\bar{g}
13.388 pb	17.6117 pb	17.6117 pb	-4.2237 pb

while eq. (3.26) and eq. (3.27) are met, eq. (3.25) is not met suggesting that mass corrections for this case can be negligible. This in turn suggests that while doped scheme, for this process, may be advantageous for differential distribution, for total cross sections the 5F scheme could still be preferred.

We find that however, for smaller values of the transverse momentum cut on the b -jets, mass corrections become non-negligible. This is due to the collinear singularity in the 5F scheme which is artificially regulated by this cut. In fact, as can be seen in fig. (4.2), the 5F and the doped scheme now differ in many regions, with the doped scheme in reasonable agreement with the 4F scheme. This suggests

that with this choice, mass corrections become more important than the value of α_S , which is still the correct one in the doped scheme. We therefore expect mass effects to be dominant at the level of total cross sections. This can be seen in tab. (4.2). In fact, for this choice of parameters, eq. (3.25) is met. Note that also eqs(3.26) and (3.27) are met, suggesting that in this case the doped scheme may be the most advantageous scheme to use.

4.2 $Zb\bar{b}$ production at LHC

Table 4.3: NLO cross sections for $Zb\bar{b}$ at $\sqrt{s} = 7$ TeV. Each scheme is computed at $\mu_R = \mu_F = M_Z + 2m_b$. The errors shown are the Monte-Carlo error.

NLO, $p_T^{cut} > 25$ GeV		
$\sigma^{(4F)}$	$\sigma^{(5F)}$	$\sigma^{(d)}$
21.1719 pb $\pm 0.34\%$	24.2749 pb $\pm 0.38\%$	23.2418 pb $\pm 0.37\%$
NLO, $p_T^{cut} > 5$ GeV		
$\sigma^{(4F)}$	$\sigma^{(5F)}$	$\sigma^{(d)}$
183.513 pb $\pm 0.28\%$	248.356 pb $\pm 0.95\%$	205.204 pb $\pm 0.4\%$

In fig. (4.3) we show differential distributions with respect to the b -pair invariant mass ($m_{b\bar{b}}$) the p_T of the leading b -jet and that of the Z boson for p_T of the b -jet $p_T^{cut} > 25$ GeV (results for $p_T^{cut} > 5$ GeV are shown in fig. (4.4)), while in tab. (4.3) we report numerical results for the total cross section for $Zb\bar{b}$ production. For this process, for $p_T^{cut} > 25$ GeV, we see that the 5F scheme and doped scheme are almost indistinguishable, even in the region of small invariant b -pair masses, since, as we saw in sect. (2.2) only the quark initiated diagrams for this process are affected by a collinear singularity while the dominant gluon channel is not. This suggests that the for this case the 5F scheme could be used. We therefore expect only conditions 2) and 3) (eqs.(3.26,3.27)) to be met. Indeed, this can be seen explicitly in tab. (4.4) where numerical values for $h^{(0)}$, \bar{h} , $g^{(0)}$ and \bar{g} are shown. This means that for this case the use of the doped scheme may not be so advantageous.

However, for $p_T^{cut} > 5$ GeV, mass corrections become more important (see fig. (4.4)). In this case in fact, the collinear singularity in the 5F scheme of the quark channel becomes the dominant contribution. This in turn spoils also the

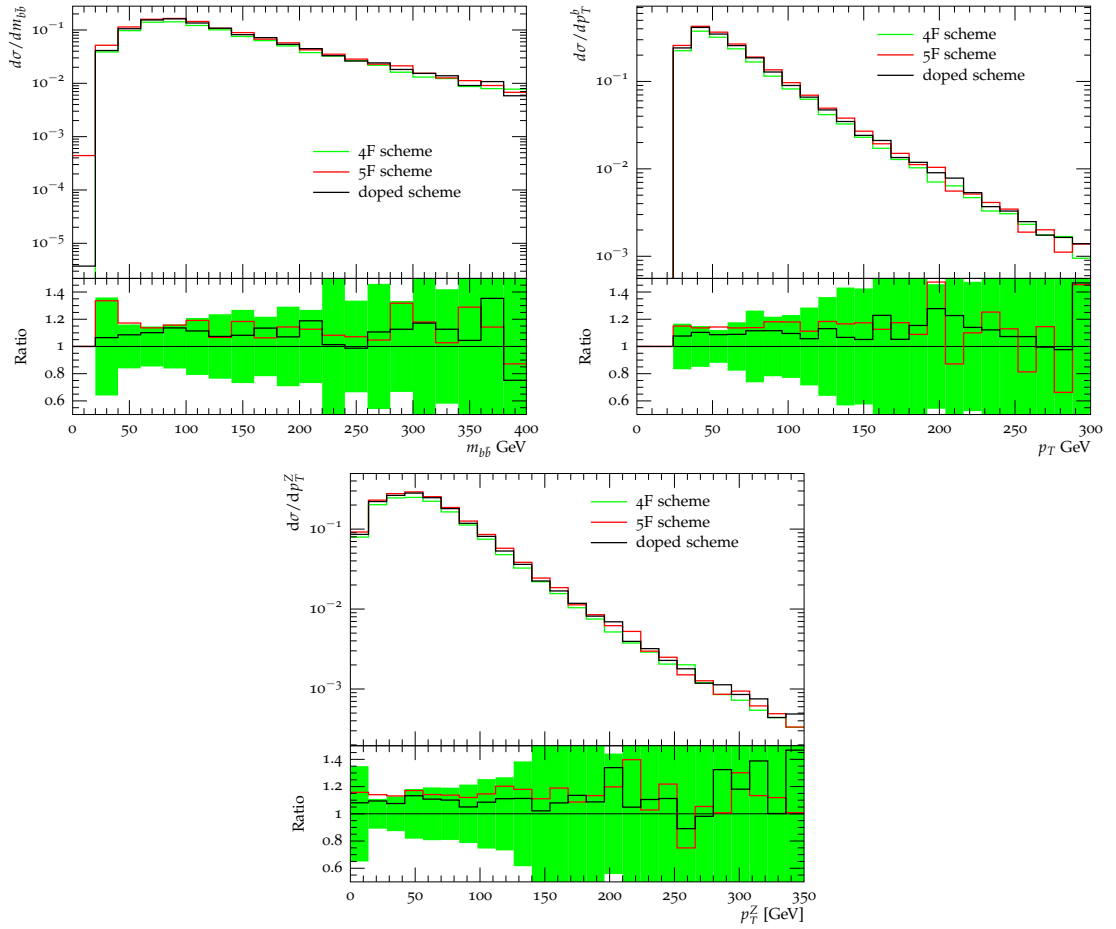


Figure 4.3: Differential distributions for $Zb\bar{b}$ production with respect to the p_T of the Z boson (bottom), of the leading p_T jet (top right) or of the invariant mass of the b -jet pair (top left), in the 4F (green), in the 5F (red) and in the doped scheme (black). The uncertainty band is that of the Monte-Carlo integration. Numerical results are obtained with $p_T^{\text{cut}} > 25$ GeV.

prediction on the total cross section in the 5F scheme. This suggests that the doped scheme may be advantageous even for this process, for this choice of the cut on the transverse momentum. We can check that this may be the case looking at tab. (4.4) where we can see that for this choice of the p_T^{cut} each condition (eqs.(3.25,3.26) and (3.27)) is met.

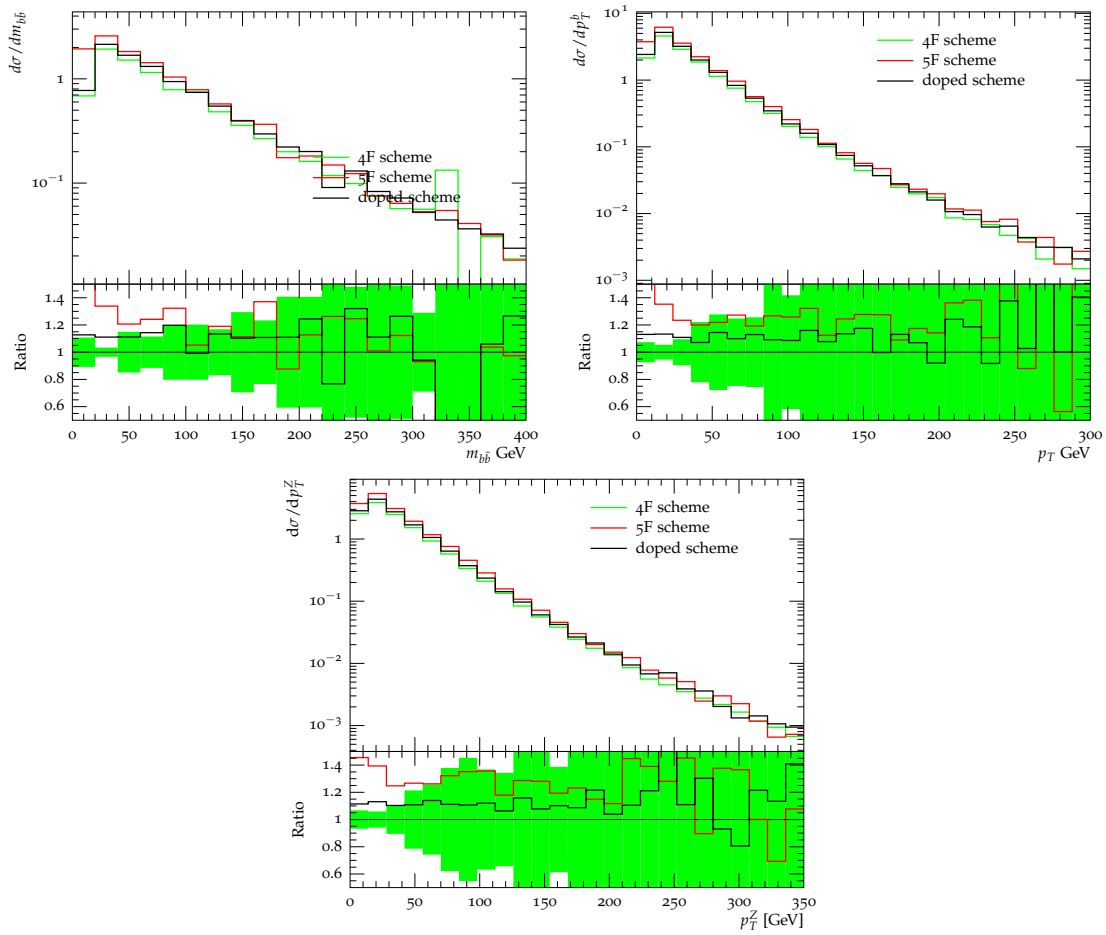


Figure 4.4: Same as fig. (4.3) but with $p_T^{cut} > 5$ GeV.

Table 4.4: $h^{(0)}, g^{(0)}, \bar{h}, \bar{g}$ values for $Zb\bar{b}$ production.

	$p_T^{cut} > 25 \text{ GeV}$		
$\Delta(5F, 4F, Q^2, \mu^2, m_b^2)$	$\Delta(5F, 4F, Q^2, \mu^2, 0)$	$h^{(0)}$	\bar{h}
3.103 pb	4.03937 pb	4.03937 pb	-0.93637 pb
<hr/>			
$\Delta(d, 4F, Q^2, \mu^2, m_b^2)$	$\Delta(d, 4F, Q^2, \mu^2, 0)$	$g^{(0)}$	\bar{g}
2.0699 pb	1.67361 pb	1.67361 pb	0.39629 pb
<hr/>			
	$p_T^{cut} > 5 \text{ GeV}$		
$\Delta(5F, 4F, Q^2, \mu^2, m_b^2)$	$\Delta(5F, 4F, Q^2, \mu^2, 0)$	$h^{(0)}$	\bar{h}
64.843 pb	27.3469 pb	27.3469 pb	37.4961 pb
<hr/>			
$\Delta(d, 4F, Q^2, \mu^2, m_b^2)$	$\Delta(d, 4F, Q^2, \mu^2, 0)$	$g^{(0)}$	\bar{g}
21.691 pb	20.0117 pb	20.0117 pb	1.6793 pb
<hr/>			

Chapter 5

A NNLO analysis

Since higher order calculations is of increasing importance in high energy physics, and since NNLO computation, in particular, are becoming more and more available, to conclude our discussion about the doped scheme we will now work out the full NNLO term which has to be subtracted in order to restore the doped scheme scale independence up to $O(\alpha_S^{N+3})$. In order to do that recall the procedure that has been used to to do the same at NLO. There we wrote:

$$(5.1) \quad \sigma^{(d)}(Q^2, \mu_R^2, \mu_F^2) = \sigma^{(d)}(Q^2, m_b^2, m_b^2) + X(Q^2, \mu_R^2, \mu_F^2),$$

where of course:

$$(5.2) \quad \sigma^{(d)}(Q^2, m_b^2, m_b^2) = \sigma^{(4F)}(Q^2, m_b^2, m_b^2) + O(\alpha_S^{N+3}).$$

Also note that we can arrange that also

$$(5.3) \quad \alpha_S^{(4F)}(m_b^2) = \alpha_S^{(d)}(m_b^2) + O(\alpha_S^3).$$

Start back then with the factorized cross section in Mellin space, eq. (2.3),

$$(5.4) \quad \sigma^{(n_f)}(Q^2) = \sum_i^{n_f} f_i^{(n_f)}(\mu_F^2) C_i^{(n_f)}(\mu_F^2, \mu_R^2, Q^2).$$

Also recall that this can be expanded in power series of the coupling constant once one uses eq. (1.30) with the result,

$$(5.5) \quad \sigma(Q^2) = \alpha_S^N(Q^2) \sum_i^{n_f} f_i(\mu_F^2) \left(C_j^{(0)} + \alpha_S(Q^2) C_j^{(1)} + \alpha_S^2(Q^2) C_j^{(2)} \right) \\ \times \left(\delta_{ij} + \alpha_S(Q^2) \Gamma_{ij}^{(1)}(\mu_F^2, Q^2) + \alpha_S^2(Q^2) \Gamma_{ij}^{(2)}(\mu_F^2, Q^2) \right) + O(\alpha_S^{N+3})$$

where

$$(5.6) \quad \begin{aligned} \Gamma_{ij}^{(1)}(\mu_0^2, \mu^2) &= \frac{1}{2\pi} \log \frac{\mu^2}{\mu_0^2} \gamma_{ji}^{(0)} \\ \Gamma_{ij}^{(2)}(\mu_0^2, \mu^2) &= \frac{1}{4\pi} \log \frac{\mu^2}{\mu_0^2} \left(2\gamma_{ji}^{(1)} + \frac{1}{2\pi} \log \frac{\mu^2}{\mu_0^2} \gamma_{jk}^{(0)} \gamma_{ki}^{(0)} - b_0 \log \frac{\mu^2}{\mu_0^2} \gamma_{ji}^{(0)} \right) \end{aligned}$$

and we dropped the n_f dependence being it trivial. Then, using eq. (1.8)

$$\alpha_S(Q^2) = \alpha_S(\mu_R^2) \left[1 - \alpha_S(\mu_R^2) b_0 \log \frac{Q^2}{\mu_R^2} + \alpha_S^2(\mu_R^2) b_0 \log \frac{Q^2}{\mu_R^2} \left(b_0 \log \frac{Q^2}{\mu_R^2} - b_1 \right) + O(\alpha_S^3) \right]$$

one obtains the full NNLO expansion. This reads, in the doped scheme

$$(5.7) \quad \begin{aligned} \sigma^{(d)}(Q^2) &= \left(\alpha_S^{(5)}(\mu_R^2) \right)^N \sum_i^{n_f} f_i^{(d)}(\mu_F^2) \left(C_i^{(0)} + \alpha_S^{(5)}(\mu_R^2) \sigma_i^{(d),(1)}(Q^2, \mu_F^2, \mu_R^2) \right. \\ &\quad \left. + \left(\alpha_S^{(5)}(\mu_R^2) \right)^2 \sigma_i^{(d),(2)}(Q^2, \mu_F^2, \mu_R^2) + O(\alpha_S^3) \right) \end{aligned}$$

with

$$(5.8) \quad \sigma_i^{(d),(1)}(Q^2, \mu_F^2, \mu_R^2) = -N b_0^{(5)} \log \frac{Q^2}{\mu_R^2} C_i^{(0)} + C_i^{(1)} + \frac{1}{2\pi} \log \frac{Q^2}{\mu_F^2} \gamma_{ij}^{(4),(0)} C_j^{(0)}$$

and

$$(5.9) \quad \begin{aligned} \sigma_i^{(d),(2)}(Q^2, \mu_F^2, \mu_R^2) &= N b_0^{(4)} \log \frac{Q^2}{\mu_R^2} \left[\frac{1}{2} (N+1) b_0^{(4)} \log \frac{Q^2}{\mu_R^2} - b_1^{(4)} \right] C_i^{(0)} \\ &\quad - (N+1) b_0^{(4)} \log \frac{Q^2}{\mu_R^2} C_i^{(1)} + C_i^{(2)} + \frac{1}{2\pi} \left(C_j^{(1)} - (N+1) b_0^{(4)} \log \frac{Q^2}{\mu_R^2} C_j^{(0)} \right) \gamma_{ij}^{(4),(0)} \log \frac{Q^2}{\mu_F^2} \\ &\quad + \frac{1}{4\pi} \log \frac{Q^2}{\mu_F^2} \left[2\gamma_{ij}^{(4),(1)} + \frac{1}{2\pi} \log \frac{Q^2}{\mu_F^2} \gamma_{ik}^{(4),(0)} \gamma_{kj}^{(4),(0)} - b_0^{(4)} \log \frac{Q^2}{\mu_F^2} \gamma_{ij}^{(4),(0)} \right] C_j^{(0)}. \end{aligned}$$

Now to compute X , as we previously did, we have to make use again of eq. (1.8),

$$(5.10) \quad \alpha_S^{(5)}(\mu_R^2) = \alpha_S(m_b^2) \left[1 - \alpha_S(m_b^2) b_0^{(5)} \log \frac{\mu_R^2}{m_b^2} + \alpha_S^2(m_b^2) b_0^{(5)} \log \frac{\mu_R^2}{m_b^2} \left(b_0^{(5)} \log \frac{\mu_R^2}{m_b^2} - b_1^{(5)} \right) + O(\alpha_S^3) \right]$$

and of eq. 1.30

$$(5.11) \quad \Gamma_{ij}^{(d)}(m_b^2, \mu_F^2) = \delta_{ij} + \alpha_S(m_b^2) \Gamma_{ij}^{(d),(1)}(m_b^2, \mu_F^2) + \alpha_S^2(m_b^2) \Gamma_{ij}^{(d),(2)}(m_b^2, \mu_F^2)$$

with

$$\Gamma_{ij}^{(d),(1)}(m_b^2, \mu_F^2) = \frac{1}{2\pi} \log \frac{\mu_F^2}{m_b^2} \gamma_{ji}^{(4),(0)}$$

(5.12)

$$\Gamma_{ij}^{(d),(2)}(m_b^2, \mu_F^2) = \frac{1}{4\pi} \log \frac{\mu_F^2}{m_b^2} \left(2\gamma_{ji}^{(4),(1)} + \frac{1}{2\pi} \log \frac{\mu_F^2}{m_b^2} \gamma_{jk}^{(4),(0)} \gamma_{ki}^{(4),(0)} - 3b_0^{(5)} \log \frac{\mu_F^2}{m_b^2} \gamma_{ji}^{(4),(0)} \right)$$

then one obtains, putting $\mu_F = \mu_R = \mu$, that:

(5.13)

$$\begin{aligned} X(\mu^2) = N \log \frac{Q^2}{\mu^2} & \left[-\frac{1}{2}(N+1) \left(\left(b_0^{(5)} \right)^2 - \left(b_0^{(4)} \right)^2 \right) \log \frac{Q^2}{\mu^2} + \left(b_0^{(5)} b_1^{(5)} - b_0^{(4)} b_1^{(4)} \right) \right] C_i^{(0)} f_i(m_b^2) \\ & + \left(b_0^{(5)} - b_0^{(4)} \right) \frac{2N+1}{4\pi} \log \frac{Q^2}{\mu^2} \gamma_{ij}^{(0)} C_j^{(0)} f_i(m_b^2) \\ & + \left(b_0^{(5)} - b_0^{(4)} \right) (N+1) \log \frac{Q^2}{\mu^2} C_i^{(1)} f_i(m_b^2) \end{aligned}$$

(5.14)

It has to be noted, however, that since,

$$(5.15) \quad \sigma^{(d)}(Q^2, \mu_R^2, \mu_F^2) = \sigma^{(d)}(Q^2, m_b^2, m_b^2) + X(Q^2, \mu_R^2, \mu_F^2)$$

and

$$(5.16) \quad \sigma^{(d)}(Q^2, m_b^2, m_b^2) = \sigma^{(4F)}(Q^2, m_b^2, m_b^2) + O(\alpha_S^{N+3}),$$

then

$$(5.17) \quad \sigma^{(d)}(Q^2, \mu_R^2, \mu_F^2) = \sigma^{(4)}(Q^2, m_b^2, m_b^2) + X(Q^2, \mu_R^2, \mu_F^2) + O(\alpha_S^{N+3}).$$

Which in turn yields that

$$(5.18) \quad \sigma^{(d)}(Q^2, \mu_R^2, \mu_F^2) = \sigma^{(4)}(Q^2, \mu_R^2, \mu_F^2) + X(Q^2, \mu_R^2, \mu_F^2) + O(\alpha_S^{N+3})$$

this means, that once one has subtracted the X term, one obtains the 4F scheme again up to higher order terms.

Chapter 6

Conclusions

In this work we proposed a hybrid scheme, called the doped scheme to account for processes in which neither the 4F scheme or the 5F scheme seem to give the most accurate prediction. This, for instance, may happen for high energy processes which start at a high perturbative order (*i.e.* with a large power of α_S), but for which mass corrections are more important than contributions from initial state logarithms arising from collinear splittings. In this cases, in fact, one should use the 4F scheme to describe correctly the whole kinematical region accessible by the process. On the other hand, since they start with a large power of α_S , the wrong value of α_S in the 4F scheme can lead to a very large error in the total cross section even for small differences between the coupling computed in the two schemes. For this reason the doped scheme was defined to be exactly equal to the 4F scheme except for the running of the coupling which is computed in the 5F scheme.

In order to obtain a fully consistent scheme up to NLO, we first had to define the doped scheme in such a way that the independence of the re-normalization scale is preserved. Once this is done, however, higher order terms receive logarithmic contributions which, though sub-leading, may in practice spoil the accuracy of the calculation. In order to assess whether this may be the case, we gave three conditions under which, if all met, the doped scheme is advantageous. We also re-expressed these conditions in term of analytically calculable quantities which can be implemented to check automatically these three conditions. Such a program has already been developed, but need a further study in order to check results obtained in this way.

We showed numerical results obtained in the 4F, in the 5F and in doped scheme for two interesting processes, namely $W/Zb\bar{b}$ production. Using these results we tried to check whether our conditions were met. We saw there that results heavily depended on the choice made on the p_T^{cut} . In fact, using a large enough value of the cut on the b -jets, the singular behavior of the 5F scheme for these two processes, is either restricted to a small region of invariant mass of the b -pair, or

is present only in a non dominant channel, resulting that the 5F scheme gives the most accurate description. When we used a smaller value of the cut imposed on the b -jets, however, we saw that mass corrections became more important, leading to the conclusion that in that case, the doped scheme was the most advantageous choice both for differential calculation and of total cross sections. We expect this behavior to be generic for processes characterized by more than one physical scale: we generally expect that there exist regions of parameters or physical scales in which the doped scheme results to be advantageous. We can therefore conclude that the doped scheme should be used or for differential analyses, when a collinear singularity in the 5F scheme spoils the accuracy in some kinematic region, or for both differential analyses and for total cross section computations when a particular range of parameters, such as p_T or pseudo-rapidity cuts, or of physical scales, makes this singular behavior more marked.

In the last part of this thesis we have computed the term which can be used to restore the scale independence of the doped scheme up to NNLO, so that this could be implemented (in principle) in a possible higher order numerical tool.

As a natural development for this work we propose to test the analytical method to check the three conditions claimed in this thesis, together with thorough test on the processes shown here and other interesting processes and physical observables.

Appendices

Appendix A

The splitting functions and the anomalous dimensions

Let us now report the full expression of the Altarelli-Parisi splitting functions with their full n_f dependence.

Remember that the splitting functions $P_{ij}(x, \mu^2)$ can be interpreted as the probability to find a parton i into a parton j with a fraction x of the longitudinal momentum of the parent parton and a trasversal momentum squared much less than the scale μ^2 . Then, each splitting function is calculable as a power series in α_S ,

$$\begin{aligned}
 P_{q_i q_j}(x, \mu^2) &= \delta_{ij} p_{qq}^{(0)}(x) + \frac{\alpha_S(\mu^2)}{2\pi} p_{q_i q_j}^{(1)}(x) + \dots \\
 P_{q_i g}(x, \mu^2) &= p_{qg}^{(0)}(x) + \frac{\alpha_S(\mu^2)}{2\pi} p_{qg}^{(1)}(x) + \dots \\
 P_{g q_i}(x, \mu^2) &= p_{gq}^{(0)}(x) + \frac{\alpha_S(\mu^2)}{2\pi} p_{gq}^{(1)}(x) + \dots \\
 P_{gg}(x, \mu^2) &= p_{gg}^{(0)}(x) + \frac{\alpha_S(\mu^2)}{2\pi} p_{gg}^{(1)}(x) + \dots
 \end{aligned}
 \tag{A.1}$$

Note that because of charge conjugation invariance and $SU(n_f)$ flavor symmetry we have

$$\begin{aligned}
 P_{q_i q_j} &= P_{q_i \bar{q}_j} \\
 P_{\bar{q}_i q_j} &= P_{q_i \bar{q}_j} \\
 P_{q_i g} &= P_{\bar{q}_i g} \equiv P_{qg} \\
 P_{g q_i} &= P_{g \bar{q}_i} \equiv P_{gq}
 \end{aligned}
 \tag{A.2}$$

Where the leading-order contribution are

$$\begin{aligned}
p_{qq}^{(0)}(x) &= \frac{4}{3} \left[\frac{1+x^2}{(1-x)_+} + \frac{3}{2} \delta(1-x) \right], \\
p_{qg}^{(0)}(x) &= \frac{1}{2} [x^2 + (1-x)^2], \\
p_{gq}^{(0)}(x) &= \frac{4}{3} \left[\frac{1+(1-x)^2}{x} \right], \\
(A.3) \quad p_{gg}^{(0)}(x) &= 6 \left[\frac{x}{(1-x)_+} + \frac{1-x}{x} + x(1-x) \right] + 2\pi \delta(1-x) b_0^{(n_f)},
\end{aligned}$$

where we used the standard plus distribution,

$$(A.4) \quad \int_0^1 dx \frac{f(x)}{(1-x)_+} = \int_0^1 \frac{f(x) - f(1)}{1-x}.$$

Alternatively one can use their Mellin transformed, the *anomalous dimensions*, γ_{ij} . They are defined as

$$(A.5) \quad \gamma_{ij}(N, \mu^2) = \int_0^{\infty} dx x^{N-1} P_{ij}(x, \mu^2).$$

then of course, they can also be expanded in power series of the coupling,

$$(A.6) \quad \gamma_{ij}(N, \mu^2) = \gamma_{ij}^{(0)}(N) + \frac{\alpha_S(\mu^2)}{2\pi} \gamma_{ij}^{(1)}(N) + \dots$$

where

$$(A.7) \quad \gamma_{ij}^{(k)}(N) = \int_0^{\infty} dx x^{N-1} p_{ij}^{(k)}(x).$$

We report here the leading-order expression reads

$$\begin{aligned}
\gamma_{qq}^{(0)}(x) &= \frac{4}{3} \left[-\frac{1}{2} + \frac{1}{N(N+1)} - 2 \sum_{i=2}^N \frac{1}{i} \right], \\
\gamma_{qg}^{(0)}(N) &= \frac{1}{2} \left[\frac{2+N+N^2}{N(N+1)(N+2)} \right], \\
\gamma_{gq}^{(0)}(N) &= \frac{4}{3} \left[\frac{2+N+N^2}{N(N^2-1)} \right], \\
(A.8) \quad \gamma_{gg}^{(0)}(N) &= 6 \left[-\frac{1}{12} + \frac{1}{N(N-1)} + \frac{1}{(N+1)(N+2)} - \sum_{i=2}^N \frac{1}{i} \right] - \frac{1}{3} n_f.
\end{aligned}$$

Appendix B

Computation of the massless limit

In this Appendix we show how the massless limit of Δ , eq. (4.3), defined in sect. (4.1) has been computed.

Let us recall that

$$(B.1) \quad \Delta(5F, 4F, Q^2, \mu^2, m_b^2) = h^{(0)} + \bar{h}$$

and

$$(B.2) \quad \Delta(d, 4F, Q^2, \mu^2, m_b^2) = g^{(0)} + \bar{g}$$

then:

$$(B.3) \quad \begin{aligned} h^{(0)} &= \Delta(5F, 4F, Q^2, \mu^2, 0), \\ g^{(0)} &= \Delta(d, 4F, Q^2, \mu^2, 0). \end{aligned}$$

In practice though $\Delta(i, j, Q^2, \mu^2, 0)$ exists only as the limit of $\Delta(i, j, Q^2, \mu^2, m_b), m_b \rightarrow 0$.

This limit in analytical form exists and is expressed, up to higher order terms, in terms of the functions a_1, a_2, a_3, d_2 as shown in sect. (3.4). One way to compute this terms is to re-write them in term of LO cross section.

In practice one can re-define those terms in the following way,

$$(B.4) \quad \begin{aligned} a_1 &= -\frac{1}{2} \frac{1}{\alpha_S^N(m_b^2)} \left(\left(b_0^{(5)} \right)^2 - \left(b_0^{(4)} \right)^2 \right) N(N+1) \sigma_{LO}(m_b^2), \\ a_2 &= \frac{1}{\alpha_S^N(m_b^2)} \sigma_{LO}^{(a_2)}(m_b^2), \\ a_3 &= \frac{1}{\alpha_S^N(m_b^2)} \sigma_{LO}^{(b)}(m_b^2), \\ d_2 &= \frac{1}{\alpha_S^N(m_b^2)} \sigma_{LO}^{(d_2)}(m_b^2). \end{aligned}$$

With:

$$\begin{aligned}
\sigma_{LO}(m_b^2) &= \alpha_S^N(m_b^2) \sum_i^4 C_i^{(0)} f_i(m_b^2), \\
\sigma_{LO}^{(a_2)}(m_b^2) &= \alpha_S^N(m_b^2) \sum_i^4 C_i^{(0)} f_i^{(a_2)}(m_b^2), \\
\sigma_{LO}^{(b)}(m_b^2) &= \alpha_S^N(m_b^2) C_b^{(0)} f_b^{(a_3)}(m_b^2), \\
\text{(B.5)} \quad \sigma_{LO}^{(d_2)}(m_b^2) &= \alpha_S^N(m_b^2) \sum_i^4 C_i^{(0)} f_i^{(d_2)}(m_b^2)
\end{aligned}$$

and

$$\begin{aligned}
\text{(B.6)} \quad f_i^{(a_2)}(m_b^2) &= \frac{1}{4\pi} \left(b_0^{(5)} - b_0^{(4)} \right) \left[\left(2\pi b_0^{(5)} - \gamma_{gg}^{(0)} \right) f_g(m_b^2) - (2N-1) \sum_i \gamma_{ji}^{(0)} f_j(m_b^2) \right], \\
f_b^{(a_3)}(m_b^2) &= \frac{1}{8\pi^2} \gamma_{gq}^{(0)} \left(2\gamma_{qq} - 6\pi b_0^{(5)} + \gamma_{gg}^{(0)} \right) f_g(m_b^2), \\
\text{(B.7)} \quad f_i^{(d_2)}(m_b^2) &= -\frac{(2N-1)}{4\pi} \left(b_0^{(5)} - b_0^{(4)} \right) \sum_i \gamma_{ji}^{(0)} f_j(m_b^2).
\end{aligned}$$

Now, as it was reported in sect. (3.4),

$$\begin{aligned}
\Delta(5F, 4F, Q^2, \mu^2, 0) &= \alpha_S^{N+2}(m_b^2) \log^2 \frac{\mu^2}{m_b^2} (a_1 + a_2 + a_3) + O(\alpha_S^{N+3}), \\
\text{(B.8)} \quad \Delta(d, 4F, Q^2, \mu^2, 0) &= \alpha_S^{N+2}(m_b^2) \log^2 \frac{\mu^2}{m_b^2} (a_1 + d_2) + O(\alpha_S^{N+3}).
\end{aligned}$$

This is the method, which has been already implemented but still need to be checked, to check the three conditions claimed for the doped scheme.

However, one can of course try to compute this limit in a numerical way. This can be achieved by computing the cross section for smaller and smaller value of the b -mass, for different values of the various parameters, such as p_T cuts and so on, interpolating Δ as a function of m_b and then taking its limit as $m_b \rightarrow 0$.

In the case considered we computed $\sigma^{(n_f)}(Q^2, m_b^2)$ at NLO, with the same cuts as that used throughout this work, for four different values of the b -mass. The results of those simulations are reported in tabs.(B.1) and (B.2). We then fitted

the function Δ between the 5F and the 4F scheme and between the doped and the 4F scheme with a polynomial of degree 4,

$$(B.9) \quad \Delta(i, j, Q^2, m_b^2) = a_{ij} + b_{ij}m_b + c_{ij}m_b^2 + d_{ij}m_b^3 + e_{ij}m_b^4$$

of course then, the massless limit is the coefficient a_{ij} .

Table B.1: $\Delta(i, j, Q^2, m_b^2)$ at NLO for $p_T^{cut} > 25$ GeV

$Wb\bar{b}$		
	$\Delta(5F, 4F, Q^2, \mu^2, m_b^2)$	$\Delta(d, 4F, Q^2, \mu^2, m_b^2)$
$m_b = 4.62$ GeV	2.1634 pb	1.7298 pb
$m_b = 0.5$ GeV	1.5988 pb	1.8878 pb
$m_b = 0.3$ GeV	1.6123 pb	2.0198 pb
$m_b = 0.1$ GeV	1.545 pb	1.8693 pb
$Zb\bar{b}$		
	$\Delta(5F, 4F, Q^2, \mu^2, m_b^2)$	$\Delta(d, 4F, Q^2, \mu^2, m_b^2)$
$m_b = 4.62$ GeV	3.103 pb	2.0699 pb
$m_b = 0.5$ GeV	3.4962 pb	2.2303 pb
$m_b = 0.3$ GeV	3.4244 pb	2.0735 pb
$m_b = 0.1$ GeV	3.7344 pb	1.8295 pb

Table B.2: $\Delta(i, j, Q^2, m_b^2)$ at NLO for $p_T^{cut} > 5$ GeV

	$Wb\bar{b}$	
	$\Delta(5F, 4F, Q^2, \mu^2, m_b^2)$	$\Delta(d, 4F, Q^2, \mu^2, m_b^2)$
$m_b = 4.62$ GeV	71.221 pb	13.388 pb
$m_b = 0.5$ GeV	19.609 pb	20.363 pb
$m_b = 0.3$ GeV	17.798 pb	19.558 pb
$m_b = 0.1$ GeV	17.313 pb	19.641 pb
	$Zb\bar{b}$	
	$\Delta(5F, 4F, Q^2, \mu^2, m_b^2)$	$\Delta(d, 4F, Q^2, \mu^2, m_b^2)$
$m_b = 4.62$ GeV	64.843 pb	21.691 pb
$m_b = 0.5$ GeV	25.836 pb	25.908 pb
$m_b = 0.3$ GeV	29.639 pb	24.327 pb
$m_b = 0.1$ GeV	29.222 pb	21.717 pb

Acknowledgements

A very special thank, of course, goes to Stefano Forte who helped me throughout this work in this year-time of work. This includes the many helpful discussions and the patience proofed (especially during writing time!).

I would also very much to thank Stefano Pozzorini, Fabio Cascioli and Niccolò Moretti of the University of Zurich in which part of this thesis has been done. Thank you very much, indeed for the whole time I made you spent on me!

Bibliography

- [1]
- [2] F.D. Aaron et al. *Combined Measurement and QCD Analysis of the Inclusive e^+p Scattering Cross Sections at HERA*. *JHEP*, 1001:109, 2010. arxiv:hep-ph/0911.0884.
- [3] U. Aglietti. *Introduction to perturbative QCD*. 1997. arxiv:hep-ph/9705277.
- [4] M.A.G. Aivazis, John C. Collins, Fredrick I. Olness, and Wu-Ki Tung. *Lep-toproduction of heavy quarks. 2. A Unified QCD formulation of charged and neutral current processes from fixed target to collider energies*. *Phys.Rev.*, D50:3102–3118, 1994. arxiv:hep-ph/9312319.
- [5] S. Alekhin, J. Blumlein, and S. Moch. *Parton Distribution Functions and Benchmark Cross Sections at NNLO*. *Phys.Rev.*, D86:054009, 2012. arxiv:hep-ph/1202.2281.
- [6] Guido Altarelli and G. Parisi. *Asymptotic Freedom in Parton Language*. *Nucl.Phys.*, B126:298, 1977.
- [7] Richard D. Ball, Valerio Bertone, Stefano Carrazza, Christopher S. Deans, Luigi Del Debbio, et al. *Parton distributions with LHC data*. *Nucl.Phys.*, B867:244–289, 2013. arxiv:hep-ph/1207.1303.
- [8] Richard D. Ball, Valerio Bertone, Francesco Cerutti, Luigi Del Debbio, Stefano Forte, et al. *Impact of Heavy Quark Masses on Parton Distributions and LHC Phenomenology*. *Nucl.Phys.*, B849:296–363, 2011. arxiv:hep-ph/1101.1300.
- [9] Richard D. Ball et al. *Unbiased global determination of parton distributions and their uncertainties at NNLO and at LO*. *Nucl.Phys.*, B855:153–221, 2012. arxiv:hep-ph/1107.2652.

- [10] Valerio Bertone, Stefano Carrazza, and Juan Rojo. *APFEL: A PDF Evolution Library with QED corrections*. *Comput.Phys.Commun.*, 185:1647–1668, 2014. arxiv:hep-ph/1310.1394.
- [11] M. Buza, Y. Matiounine, J. Smith, and W.L. van Neerven. *Charm electro-production viewed in the variable flavor number scheme versus fixed order perturbation theory*. *Eur.Phys.J.*, C1:301–320, 1998. arxiv:hep-ph/9612398.
- [12] M. Buza, Y. Matiounine, J. Smith, and W.L. van Neerven. *Charm electro-production viewed in the variable flavor number scheme versus fixed order perturbation theory*. *Eur.Phys.J.*, C1:301–320, 1998. arxiv:hep-ph/9612398.
- [13] Matteo Cacciari, Mario Greco, and Paolo Nason. *The $P(T)$ spectrum in heavy flavor hadroproduction*. *JHEP*, 9805:007, 1998. arxiv:hep-ph/9803400.
- [14] Matteo Cacciari, Gavin P. Salam, and Gregory Soyez. *The Anti- $k(t)$ jet clustering algorithm*. *JHEP*, 0804:063, 2008. arxiv:hep-ph/0802.1189.
- [15] J.M. Campbell, F. Caola, F. Febres Cordero, L. Reina, and D. Wackerroth. *NLO QCD predictions for $W+1$ jet and $W+2$ jet production with at least one b jet at the 7 TeV LHC*. *Phys.Rev.*, D86:034021, 2012. arxiv:hep-ph/1107.3714.
- [16] F. Cascioli, S. Hche, F. Krauss, P. Maierhofer, S. Pozzorini, et al. *Precise Higgs-background predictions: merging NLO QCD and squared quark-loop corrections to four-lepton + 0,1 jet production*. *JHEP*, 1401:046, 2014. arxiv:hep-ph/1309.0500.
- [17] Fabio Cascioli, Philipp Maierhofer, Niccolo Moretti, Stefano Pozzorini, and Frank Siegert. *NLO matching for $t\bar{t}b\bar{b}$ production with massive b -quarks*. 2013. arxiv:hep-ph/1309.5912.
- [18] Fabio Cascioli, Philipp Maierhofer, and Stefano Pozzorini. *Scattering Amplitudes with Open Loops*. *Phys.Rev.Lett.*, 108:111601, 2012. arxiv:hep-ph/1111.5206.
- [19] Stefano Catani. *Aspects of QCD, from the Tevatron to the LHC*. 2000. arxiv:hep-ph/0005233.
- [20] Richard Keith Ellis, William James Stirling, and Bryan R Webber. *QCD and Collider Physics*. Cambridge monographs on particle physics, nuclear physics, and cosmology. Cambridge Univ. Press, Cambridge, 2003. Photography by S. Vascotto.

- [21] Fernando Febres Cordero. *Next-to-Leading-Order Corrections to Weak Boson Production with a Massive Quark Jet Pair at Hadron Colliders*. 2007. arxiv:hep-ph/0809.3829.
- [22] Fernando Febres Cordero, L. Reina, and D. Wackerth. *W- and Z-boson production with a massive bottom-quark pair at the Large Hadron Collider*. *Phys.Rev.*, D80:034015, 2009. arxiv:hep-ph/0906.1923.
- [23] Stefano Forte, Eric Laenen, Paolo Nason, and Juan Rojo. *Heavy quarks in deep-inelastic scattering*. *Nucl.Phys.*, B834:116–162, 2010. arxiv:hep-ph/1001.2312.
- [24] Stefano Forte, Lorenzo Magnea, Andrea Piccione, and Giovanni Ridolfi. *Evolution of truncated moments of singlet parton distributions*. *Nucl.Phys.*, B594:46–70, 2001. arxiv:hep-ph/0006273.
- [25] T. Gleisberg, Stefan. Hoeche, F. Krauss, M. Schonherr, S. Schumann, et al. *Event generation with SHERPA 1.1*. *JHEP*, 0902:007, 2009. arxiv:hep-ph/0811.4622.
- [26] Marco Guzzi, Pavel M. Nadolsky, Hung-Liang Lai, and C.-P. Yuan. *General-Mass Treatment for Deep Inelastic Scattering at Two-Loop Accuracy*. *Phys.Rev.*, D86:053005, 2012. arxiv:hep-ph/1108.5112.
- [27] S. Haywood, P.R. Hobson, W. Hollik, Z. Kunszt, G. Azuelos, et al. *Electroweak physics*. 1999. arxiv:hep-ph/0003275.
- [28] 1 Kramer, Michael, Fredrick I. Olness, and Davison E. Soper. *Treatment of heavy quarks in deeply inelastic scattering*. *Phys.Rev.*, D62:096007, 2000. arxiv:hep-ph/0003035.
- [29] Hung-Liang Lai, Marco Guzzi, Joey Huston, Zhao Li, Pavel M. Nadolsky, et al. *New parton distributions for collider physics*. *Phys.Rev.*, D82:074024, 2010. arxiv:hep-ph/1007.2241.
- [30] Fabio Maltoni, Giovanni Ridolfi, and Maria Ubiali. *b-initiated processes at the LHC: a reappraisal*. *JHEP*, 1207:022, 2012. arxiv:hep-ph/1203.6393.
- [31] A.D. Martin, W.J. Stirling, and R.S. Thorne. *MRST partons generated in a fixed-flavor scheme*. *Phys.Lett.*, B636:259–264, 2006. arxiv:hep-ph/0603143.
- [32] A.D. Martin, W.J. Stirling, R.S. Thorne, and G. Watt. *Parton distributions for the LHC*. *Eur.Phys.J.*, C63:189–285, 2009. arxiv:hep-ph/0901.0002.

-
- [33] Antonio Pich. *Aspects of quantum chromodynamics*. pages 53–102, 1999. arxiv:hep-ph/0001118.
- [34] Peter Skands. *Introduction to QCD*. 2012. arxiv:hep-ph/1207.2389.
- [35] R.S. Thorne. *A Variable-flavor number scheme for NNLO*. *Phys.Rev.*, D73:054019, 2006. arxiv:hep-ph/0601245.
- [36] R.S. Thorne and R.G. Roberts. *An Ordered analysis of heavy flavor production in deep inelastic scattering*. *Phys.Rev.*, D57:6871–6898, 1998. arxiv:hep-ph/9709442.
- [37] Wu-Ki Tung, Stefan Kretzer, and Carl Schmidt. *Open heavy flavor production in QCD: Conceptual framework and implementation issues*. *J.Phys.*, G28:983–996, 2002. arxiv:hep-ph/0110247.
- [38] A. Vogt. *Efficient evolution of unpolarized and polarized parton distributions with QCD-PEGASUS*. *Comput.Phys.Commun.*, 170:65–92, 2005. arxiv:hep-ph/0408244.